BIOSYNTHESIS OF ZINC OXIDE NANOPARTICLES EMPLOYING FRUITS PEEL WASTE AND THEIR EFFICIENCY FOR DEGRADING MALACHITE GREEN DYE

Thesis

Submitted to the

G. B. Pant University of Agriculture & Technology
Pantnagar- 263145, Uttarakhand, India

By

Deepak Bahuguna
Id. No. 55546

IN PARTIAL FULFILLMENT OF THE REQUIREMENTS FOR THE DEGREE OF

Master of Science
(Environmental Science)

September, 2021

ACKNOWLEDGEMENT

Writing this thesis has been fascinating and extremely rewarding. I would like to thank a number of people who have contributed to the final consequence in many different ways. To commence with, I pay my obeisance to GOD, the almighty to have bestowed upon me good health, courage, zeal, illumination, strength and patience. I hereby, express my profound sense of gratitude to my Advisor Dr. Shweta Saraswat, Assistant Professor, Department of Environmental Science and chairman of my advisory committee, for her guidance, motivation, help and standing beside me through really tough times. Her expertise, invaluable guidance, constant encouragement, affectionate attitude, understanding, patience and healthy criticism added considerably to my learning.

I wish to express my gratitude to the esteemed members of my advisory committee, Dr. R.K. Srivastava, Professor and Head, Department of Environmental Science and Dr. Sneh Gautam, Assistant Professor, Department of Molecular Biology And Genetic Engineering.

It is a privilege to express my heartiest regards and sincere thanks to the entire faculty members Dr. R.K. Srivastava, Dr. J.P.N. Rai, Dr. Vir Singh, and Dr. Uma Melkania for their cooperation and support throughout the degree programme. I also acknowledge a deep thanks to all the support staff members Shweta ma'am, Akram sir, Manoj Sir, Nageshwar sir, Gupta sir and others for their day to day help in research work by providing all essential help during the studies.

I also owe great thanks to Dean, PGS and Dean, CBSH for providing necessary facilities during the pursuit of my research work.

I would like to acknowledge all the teachers I learnt from since my childhood, I would not have been here without their guidance, blessing and support.

Where the emotions are involved, words cease to mean. My vocabulary fails to accentuate my profound reverence and sincere regards to my grandparents and to my parents, my source of inspiration, encouragement Mr. Puran Chandra and Mrs. Janki Devi who raised me with love, supported me so far, believe in me, and guiding me to achieve success at every step of life and in all my pursuits. I have special words of thanks from the core of my heart to my loving sibling Jagdish and other family

members and my friends Preet, Vinay, Shivik and Tanya for their unconditional love, affection and care. I owe everything to my family.

The help and guidance provided by my PhD seniors Arjita ma'am, Anamika ma'am, Moumita ma'am, Monika ma'am, Shivam sir, Diksha ma'am, Ankita ma'am, Shushmita ma'am, and Nikhil sir and their supportive attitude mingled with care I received, is deeply acknowledged. I am grateful to my M.Sc. seniors, Diksha ma'am, Prayanjali ma'am, Alisha ma'am, Akhil sir, Nandini ma'am, and Prabhakaran sir for the stimulated discussion warm company, love and care. There are no words to pay my regards to many unforgettable persons during my stay in Pantnagar.

I sincerely admire the contribution of Ananya, Debjyoti and Milan and of my classmates Indu, Ashutosh Pandey, Hema Kandpal, Vandana Pachhai, Vandana Arya and Sultan for their pleasant company, co-operation, help and for those memorable moments, which will always be remembered. Words are limited to express the contribution and active help given by them.

I am also grateful to all my loving juniors Shifa, Pratibha, Divya and Sonali for their active help. A very special thanks to my friends Kamal, Himanshu, Moin, Arun, Pawnesh, Rajneesh, Abhishek, Sangeeta, Aabha, Akanksha, Aparna and Pratibha whose care, mischief and kind support did not ever let me feel out of my family and made my stay at Pantnagar memorable.

Lastly, I shall ever remain thankful to all those who could not have find separate names but had directly or indirectly helped me.

Thanks for all your encouragement!

Pantnagar
September, 2021

(Deepak Bahuguna)
Author

CERTIFICATE-I

This is to certify that the thesis entitled **"BIOSYNTHESIS OF ZINC OXIDE NANOPARTICLES EMPLOYING FRUITS PEEL WASTE AND THEIR EFFICIENCY FOR DEGRADING MALACHITE GREEN DYE"** submitted in partial fulfillment of the requirements for the degree of **Master of Science** with major in **Environmental Science** of the College of Post Graduate Studies, G.B. Pant University of Agriculture and Technology, Pantnagar, is a record of bonafide research carried out by **Mr. Deepak Bahuguna** Id. No. **55546,** under my supervision, and no part of the thesis has been submitted for other degree or diploma.

The assistance and help received during the course of this investigation have been duly acknowledged.

(Shweta Saraswat)
Chairperson
Advisory Committee

Pantnagar
September, 2021

CERTIFICATE-II

We, the undersigned, members of the Advisory Committee of **Mr. Deepak Bahuguna**, Id. No. **55546**, a candidate for the degree of **Master of Science** with major in **Environmental Science**, agree that the thesis entitled **"BIOSYNTHESIS OF ZINC OXIDE NANOPARTICLES EMPLOYING FRUITS PEEL WASTE AND THEIR EFFICIENCY FOR DEGRADING MALACHITE GREEN DYE"** may be submitted in partial fulfilment of the requirements for the degree.

(Shweta Saraswat)
Chairperson
Advisory committee

(R.K. Srivastava)
Member

(Sneh Gautam)
Member

CONTENTS

LIST OF TABLES

LIST OF FIGURES

LIST OF ABBREVIATIONS

%	Percentage
a.u.	Absorbance units
Caltech	California Institute of Technology
Conc.	Concentration
CPF	Chlorpyrifos
DBT	Dibenzothiophene
DETP	Diethyl thiophosphate
DLS	Dynamic light scattering
EBT	Eriochrome Black T
EDS	Energy dispersive spectroscopy
FTIR	Fourier Transform Infrared
GNP	Graphene nanoparticle
KZnHCF	potassium zinc hexacyanoferrate
MFP	Mixed fruit peel
MG	Malachite Green
NBPs	Nanobioparticles
NPs	Nanoparticles
OP	Organophosphorus pesticide
pH	Potential of hydrogen
ppm	Parts per million
ppt	Precipitate
PXRD	Powdered X-ray diffraction
SEM	Scanning Electron Microscopy
SNP	Silver nanoparticles
TCP	3, 5, 6-trichloropyridinol

TEM	Transmission electron microscopy
TFC	Total flavonoid content
TPC	Total phenolic content
TTC	Total tannins content
XRD	X-ray diffraction
ZnO	Zinc oxide
ZnO NPs	Zinc oxide nanoparticles

Introduction

Chapter 1 INTRODUCTION

Intensive urbanization, industrialization, as well as population pressure on finite natural resources and, to a lesser extent, natural activity, have all put an enormous strain on the global environment through releasing harmful toxins. One of the most serious environmental issues is water contamination. Textile, leather and paper industries release anthropogenic substances such as malachite green and methylene blue etc., which contaminate both surface and ground water sources. Every year 280000 tons of dyes are used by the dyeing industries and are discharged directly into the stream. Malachite Green (MG) is used as a coloring agent by food, wool, paper, jute, cotton, leather, and acrylic (as an additive) industries. Malachite green has been in controversy due to its toxicity for all the living organisms. Malachite green is extremely carcinogenic and can cause cancer and mutagenicity in many species such as fish, algae, and bacteria. The dyes also hinders the penetration of sunlight in aquatic system and also cause myriads of other diseases in living organisms even at low concentration. Fishes treated with malachite green have shown its carcinogenic effects on immune and reproductive system.

Nanotechnology has become one of the fastest emerging field of modern sciences which provides the platform to design, construct and manipulate the nanoparticles for removal of dyes from the varied nature of waste waters. Nanoparticles may help in removal of dyes specifically as being target specific, non-toxic and cost effective in nature. The nanoparticles produced through various physical and chemical processes cause many environmental related problems. As the Physical and chemical methods are hazardous, laborious and non-ecofriendly, there is an urgent need to explore nanoparticles that can be produced biologically and are less harmful for the environment **(Saratale *et al.*, 2018).**

1.1 'Green waste' – values and scope

Green waste (food, agro-industrial, and forest leftovers) is a well-known polyphenol source. Their unique properties of chelation, adsorption, reduction,

complexation, nutrient cycling, antimicrobial activities and plant growth, makes them an excellent natural and relatively effective agents of cleaning environmental toxins. Existing bio-remedial techniques such as biosorption, phytoextraction, and coagulation have found effective in the removal of heavy metals, pathogenic microbes and dyes from contaminated soil and water. Polyphenol-rich natural extracts are increasingly being used in green nanoparticle synthesis (in the manufacture of particles between 1 and 100 nanometers in size) utilizing biological entities (such as microbes or plant biomass) as a therapeutic agent in the detoxification of harmful contaminants. Current bioremediation methods, on the other hand, are not fully naturally derived.

Therefore there is an urgent need to synthesize eco-friendly nanoparticles by utilizing biogenic products that are non- toxic, easily degradable and have regenerative capabilities too. Green synthesis of nanoparticles employs green methodology and the chemicals that are used during the synthesis process are not harmful. Moreover, the process of green synthesis can be performed at normal room temperature and pressure. Green synthesis is the utilization of biological agents including plants part extract, microbes, agro-industrial waste (fruits and vegetable peel waste) and others. Formation of nanoparticle using green synthesis method is stable, simple, rapid, cost-effective, ecofriendly and non-toxic **(El-Gendy *et al.*, 2019)**.

1.2 Green waste as renewable polyphenol source

Phenols are a collection of phytochemicals that can be found in all of plant's vegetative organs and subsequently preserved in dead plant parts found in green waste. Plant phenolic compounds are responsible for 40% of all organic carbon in the biosphere. Chemically, phenolic compounds are defined with at least one aromatic ring with one (phenol) or more (polyphenols) hydroxyl substituents, as well as their functional derivatives (e.g., glycosides and esters). Polyphenols are water soluble compounds with a molecular mass of 500 to 4,000 Dalton possessing 12 to 16 phenolic hydroxyl groups and 5 to 7 aromatic rings per 1,000 Dalton, according to **Haslam *et al.* (2010).**

Furthermore, Low and high molecular weight substances, such as phenolic acids and lignin, are classified as (poly) phenols. The most crucial class of polyphenols is phenolic acids, which includes polymeric structures such as lignans, stilbenes, hydrolysable tannins, and flavonoids. Flavonoids include flavones, isoflavones, flavanones, anthocyanidins (pigments responsible for the color in most fruits), flavanols (the most common flavonoids in food, such as quercetin and kaempferol). These polyphenols are primarily produced by nature in plants by the shikimate or malonate secondary metabolite pathways, or both. Thousands of polyphenols (almost 8,000) have been identified and linked to variety of health benefits, because of their biological qualities, such as antioxidant, anticancer, and anti-inflammatory, catalytic degradation capabilities and in chemical defense mechanism.

Polyphenols' ability to scavenge free radicals, bind metal ions, and contribute hydrogen atoms or electrons are the key functional features. Bioavailability, molecular size, stability and the ability of polyphenols to conjugate with other phytochemicals or phenolic compounds, are all important factors in their functional activity. The activity of phenolic compounds is determined by the number and position of hydroxyl groups in respect to carboxyl functional groups. Emerging findings suggest that there are various potential mechanisms of action by which polyphenols may promote bioremediation owing to their metal chelation and radical stabilization activities **(Skapin *et al.*, 2007).** Before understanding the remedial opportunities offered by polyphenols, it is important to understand the source, availability and variations in concentration of polyphenols in natural wastes.

1.3 Sources of Polyphenols

1.3.1. Food and agro-industrial waste

Almost all types of food and agro-industrial leftovers (fruits, vegetables, oilseeds, nuts, cereals and beverages) include polyphenols. The main sources of these wastes are industries and households. Polyphenols have been found in a variety of foods and beverages. Rice (*Oryza sativa*) husk **(Tripathi *et al.*, 2014),** peanut hulls,

(*Arachis hypogaea*) hulls **(Nair *et al.*, 2002),** hazelnut (*Corylus avellana*) shells **(Azizi *et al.*, 2014),** leftover coffee grounds (*Coffea arabica*) **Nagarajan *et al.*, 2013,** apple pomace (*Malus sp.)* **(Dobrucka *et al.*, 2016)** and a variety of other wastes.

Gorinstein *et al.*, (2014) found 15% higher total polyphenolic content in peel of citrus fruits (oranges - *Citrus sinensis* and lemons – *Citrus limon*) than those in the peeled fruits. Since, the citrus industry produces large quantities of peel and seed residues, which account for nearly 50% of the total fruit weight, with maximum phenols, they can be considered as a potential source of polyphenols. Nutshells and residues from fruit juice production, notably peels and pomace, contain comparatively high amounts of total polyphenols in contrast to dried minor residues obtained from agro-food-industries and forest debris.

1.3.2. Forest and garden waste

It is important to note that, among green wastes, forest and garden wastes haven't been thoroughly investigated as phenolic compounds sources. Fresh tree leaves, on the other hand, have lately been examined for their polyphenolic content and are commonly used for green nanoparticle production due to stabilizing, capping, and reducing potentials of polyphenols **(Fu *et al.*, 2015).** The principal polyphenolic elements of forestry wastes include flavonoids and tannins.

According to **Sultana *et al.*, (2015)** the bark of Neem (*Azadirachta indica*), Babul (*Acacia nilotica*), and Arjun (*Terminalia arjuna*) trees contains a total polyphenolic content of 7.8-16.5 mg/g^{-1}, with flavonoids alone accounting for 75% of the total polyphenolic content. Eucalyptus (*Eucalyptus sp*.) bark contains 0.11-0.22 mg/g^{-1} of total phenols, 2.48% lignin, 41.63% cellulose, and 62.47% total sugars, according to **Vazquez *et al.*, (2016).**

Polyphenolic concentrations in dry residues from cultivation or harvesting activities from trees within and around of forests, orchards, and landscape management (including residential and urban green areas) are yet unknown. This is especially important as phenolic chemicals are abundant in forestry wastes as well as agro-industrial residues, and if further investigated, could have practical significance.

Other methods of producing nanoparticles includes chemical reduction via different organic and inorganic reducing agents, electrochemical techniques, irradiation method, mechanical grinding etc. **(Choi *et al.*, 2011).** Nanoparticles based on metals like zinc, copper, silver, titanium, iron, gold etc., can be produced by various physical and chemical methods within the range of 1-100nm **(Sukri *et al.*, 2019).** In earlier studies, successful attempts have been made to degrade cationic dyes by Ag-nanoparticles using fruit waste**,** degradation of congo red dye using ZnO nano-photocatalyst using Artocarpus leaves extract etc**.**

1.4 Zinc oxide nanoparticles

Metal oxide nanoparticles synthesis through green synthesis method has been a highly lucrative research area over last decade. Various biocomponents like bacteria, fungi, plant extract are promising source of substrates used in the fabrication of nano materials. Out of various options Plant extract based synthesis is preferred for the controlled nanoparticles synthesis (shape, size and other specific feature). Also the growing, extensive usage of dyes in textile, paper and other industries are growing concern for environmentalist over the globe. ZnO nanoparticles is a white powder which is nearly soluble in water. It has been widely used in various materials and products including glass, paints, adhesive, food supplements (Zn nutrients), fire retardants etc. Naturally occurring zinc oxide mineral “zincite” is quite rare in earth’s crust. The color of the zincite depends on the impurities that it possess. As zincite is rare, most of the commercially usage of zinc oxide is fulfilled by synthetic production. Zinc oxide is non-toxic to human skin which makes it suitable accompaniment for textile usage.

1.4.1. Importance of zinc oxide nanoparticle

1. It can be used in pharmaceutical products, plastic and rubber manufacturing, cosmetics, food supplements, skin care products etc.
2. ZnO nanoparticles are found to be useful in the treatment of leukemia and carcinoma.
3. It shows strong antibacterial properties.

4. It is used in the degradation of various hazardous dyes.
5. It is non-toxic to humans.
6. It is also used as a drug carrier.

Properties of nanomaterial like high surface area, high thermal and electrical conductivity, antimicrobial, biocompatibility and catalytic property to disintegrate organic material are responsible for their diverse usage. The large band gap (about 3.37eV) & exciton binding energy 60meV **(Hadia *et al.*, 2014)** of ZnO semiconductor reduces its size and also affects its conductivity. The 3.1-3.3 eV band gap of zinc oxide has been used in various applications, such as biosensors, drug carrier, antibacterial agent, cosmetics etc. The biocompatibility and the catalytic and reductive property of Zinc oxide nanoparticles (ZnO-NPs) makes it a good choice for waste water treatment. ZnO-NPs can be used in degradation of pesticides **(Khan *et al.*, 2020)**, dyes **(Sukri *et al.*, 2019)**, adsorption of heavy metals **(Hadadian *et al.*, 2018)** etc.

Further, global fruit production has experienced a remarkable spike in recent years. India stood 2nd in production of fruit after china (2017-18). During 2017-18, India produced 97.2 million metric tons of fruits, as per national horticulture database published by National Horticulture Board. Due to low shelf life and seasonal availability, the fruits are usually processed in the form of bottled juices, pickles, dried, jellies etc., to increase their life. This generates huge amount of waste and if not managed causes various environmental problems. These organic waste can also be utilized to generate bio-nanoparticles for the removal of dyes. To keep this in view, the present study has conducted to synthesis and characterize ZnO-NPs using multiple fruit peel waste of pomegranate, banana, grapes, oranges and apples has done using various techniques like UV-visible spectroscopy, dynamic light scattering (DLS), X-ray diffraction (XRD), Fourier transform infra-red spectroscopy (FT-IR) and scanning electron microscope (SEM). Furthermore, the evaluation of cationic dye degradation property of synthesized nanoparticles has also been observed.

Considering the above mentioned facts, the present work had been planned to achieve the following objectives:

1. Synthesis of zinc oxide nanoparticles via green synthesis, employing fruits peel waste.
2. Surface and chemical characterization of synthesized zinc oxide nanoparticles.
3. Investigation and optimization of malachite green (dye) removal efficiency of mixed fruit peel derived zinc oxide nanoparticles at varying pH, dye concentration, nanoparticles dose and time interval.

Review of Literature

"K. E. Drexler" is known as the father of nanotechnology. He was the one who explained the subject of nanotechnology in depth and thus played a main role in popularizing the subject. There are various products of nanotechnology, such as nanotube, nano filters, nanoparticles, nanospheres etc., that are used in different sectors like food processing, pharmacology, waste water treatment, targeted therapy, nano-sensors, nanocoating etc. Along with the benefits that nanoparticles offers, they pose immense potential for the removal of various environmental contaminants, which is the primary concern of mankind **(Choi *et al.*, 2011).** It has the potential to contribute in the long-term water quality related issues. Various treatment technologies have made immense development in past few years in handling the contaminated waste water, using nanotechnology.

Although their production through various physical and chemical processes cause many environmental problems such as disposal of nano-contaminants and nano-wastes. On the other hand the green synthesis of nanoparticles is environment friendly, easy to manage and non-toxic method. In green synthesis, the biological extract is used as a reducing agents to reduce the precursor metal compound to metal nanoparticles. Compounds like flavonoids, alkaloids, phenols and polyphenols obtained from plant part (leaves, fruit etc.) extract act as reducing agents. In previous studies, different plants part extract have also been used in degradation and removal of various environmental pollutants **(Saratael *et al.*, 2018).**

2.1 Approaches for synthesis of nanoparticles

Metal nanoparticles is an active area of applied research in nanotechnology, mainly because of their large surface area and capability to transfer electrons from donor to acceptors. There are various methods of synthesizing nanoparticles. These technologies use "Top-Down" and "Bottom-Up" approaches.

2.1.1 Top- down Approach

In “Top Down” approach (destructive approach), nanoparticles are reduced in size using various physical and chemical methods. Attrition and milling are the two most common methods of making nanoparticles using top down method. In top-down approach milling, cutting and shaping methods are used to mold the material into desired model and micro-fabrication **(figure 2.1).**

Photolithography and inkjet printing are the techniques included in micro-patterning. The most common approach in top-down method starts with the selection of appropriate material and then shaping the functionality from inner material. This method is similar to the method used in semiconductor industries, for the synthesis of devices having silicon, copper etc. Another method is laser pyrolysis, an easy and effective method of synthesizing nano powders. The energy current between the carbon dioxide laser and the reagent increase the temperature in the reactive zone and cause vibration of molecules. The above method is simple way of particle synthesis in the range of 15-20 nm. Ionic/electronic irradiation, etching, mechanical milling and sputtering are few another ways of producing nanoparticle, using top down approach **(Jamkhande *et al.*, 2019).**

2.1.2 Bottom-Up Approach

In bottom-up approach (constructive method) the nanoparticles are synthesis employing small entities, such as atoms and molecules, for which the oxidation/reduction reactions are the main proponents. Bottom-up approach in comparison, utilize chemical characteristics of individual substances to form product. It involves different methods like supercritical fluid, sol gel technique, atomic condensation, electrochemical precipitation, vapor deposition etc. Biological system is found to be suitable for this approach, in which the chemical components of life act as reducing and stabilizing agents to carry out the production of nanoparticles with minimum defect and homogenous composition **(De Oliveira *et al.*, 2018)**

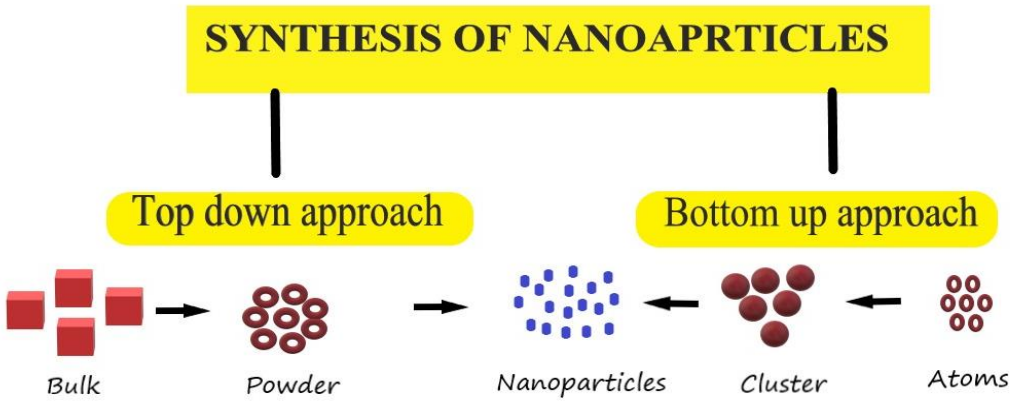

Figure 2.1: Top-down and Bottom-up approaches of nanoparticles synthesis.

2.2 Synthesis of Zinc Oxide nanoparticles

Metal oxide nanoparticles can be synthesized via physical, chemical and biological methods **(figure 2.2)**. Every method has its own characters and benefits, but our focus is more on the biological way of synthesizing nanoparticles as its clean, facile and environment friendly.

Zinc oxide is of tremendous economic and industrial relevance because of its diverse qualities, which allow it to be used in a variety of industries, including the rubber sector, biomedical field, and metal surface treatment. The key properties of zinc oxide includes its semi conductivity, antibacterial activity and UV absorption. With the introduction of Nanotechnology, these qualities can be improved by increasing the surface area of the material i.e. by reducing particle size and by changing the shape.

2.2.1 Physical Methods

Physical vapor deposition, Arc plasma method, ultrasonic irradiation are some of the most popular physical methods of nanoparticle synthesis.

Yang *et al.* (2006) reviewed the synthesis of zinc nanoparticles using laser ablation of a solid target in confined liquid medium. The focus was to understand the mechanism of crystal growth. He also explained the effect of liquid confinement,

phase transition and kinetic growth of the nanocrystals. Other applications of laser ablation includes surface patterning, surface cleaning, and surface coating. Theoretical analysis and experimental results indicates that laser ablation technique of a solid target in confined liquid medium is an effective way to synthesize nanocrystals. Following are the benefits of using laser ablation technique :-

1. Chemically simple and clean.
2. Can be performed in normal conditions. High temperature and pressure is not required.
3. Novel phase formation of nanocrystals may involve both solid and liquid phase.

Submicron zinc oxide nanoparticles were successfully developed using one step aqueous precipitation method. Different morphologies such as flower and snowflakes were obtained by changing the reaction temperature. Findings of the author suggest that self-aggregation and orientation aggregation enhanced by increasing temperature could be the possible mechanism behind the formation of nanostructure. Findings also suggests different structure anomalies such as differences in mass distribution and crystalline structure. The XPS characterization revealed the presence of $Zn(OH)_2$ and absorbed carbon species ion ZnO surface. In addition, UV emission and UV excitation centered in 390 nm and 360 nm respectively, for the sample synthesized at 60°C.

Another laser ablation method of preparation of zinc oxide nanoparticles using zinc metal plate and liquid medium with different surfactant solutions such as Cationic, anionic, amphoteric and nonionic was performed by **Hiroyuki Usui *et al.* (2004)**. The nanoparticles were acquired in deionized water and in each surfactant solutions. There was a decline in the average particles size with increasing amphoteric and nonionic surfactant concentration. The quantum size of ZnO particles was reported around 7nm. Various defect emission peaks were also reported, which might be attributed to either due to impurity or lattice defects.

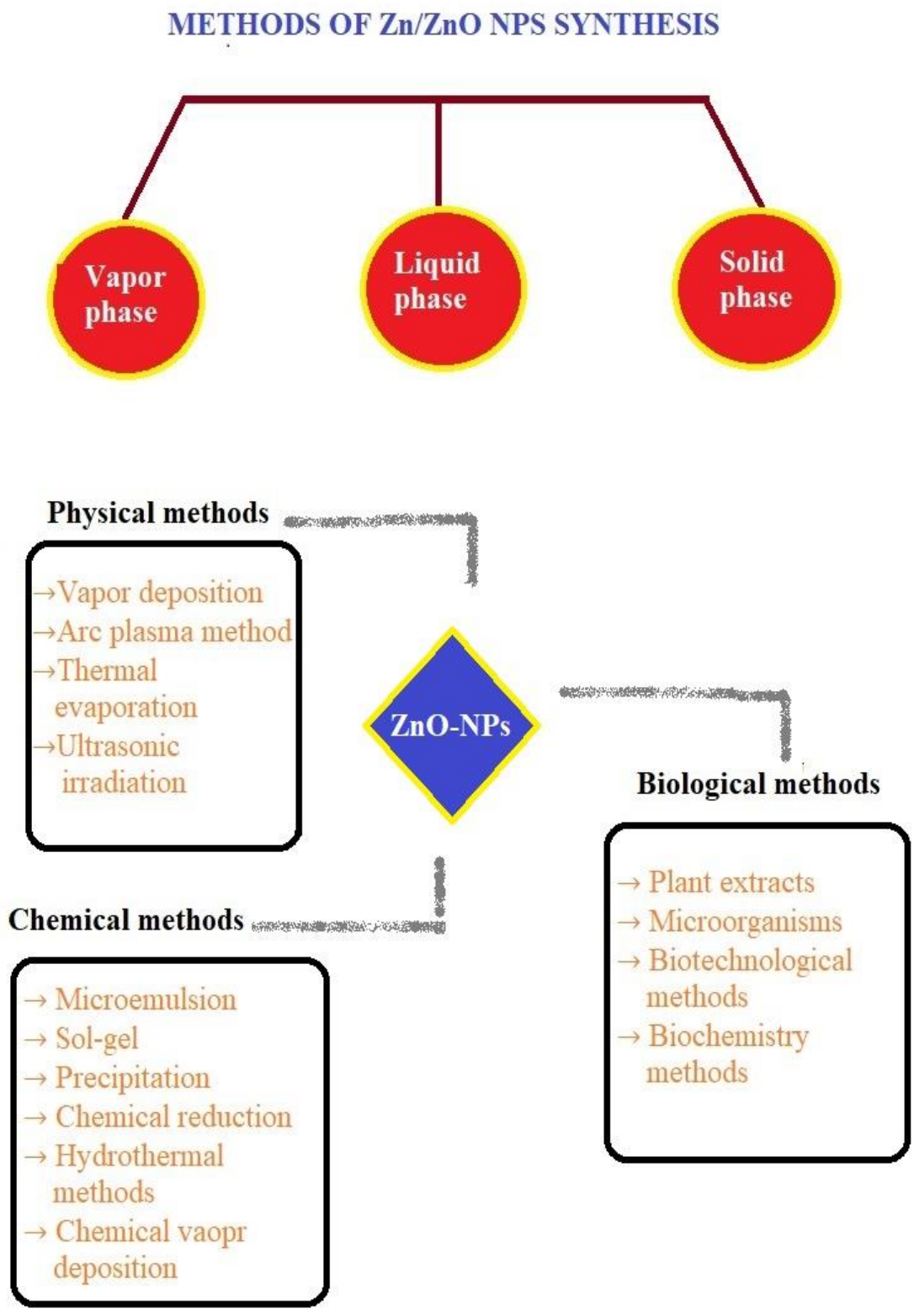

Figure 2.2: Methods of zinc oxide nanoparticles synthesis.

Wei Jin *et al.* (2007) employed chemical vapor synthesis (CVS) which is a modified form of chemical vapor deposition (CVD), for the synthesis of Cr doped ZnO nanoparticles. The obtained nanocrystalline particles were subjected to nitrogen adsorption, energy dispersive X-ray analysis (EDX) and other characterization techniques. He observed increase in particles size with increasing doping concentration. ZnO nanoparticle with mean diameter 27nm and equi-axial morphology with slight agglomeration were observed. The maximum accumulation of Cr was found partially on the distorted tetrahedral site and the reason behind the formation of distorted sites might be due to segregation of chromium atom to the particle surface.

Marco stoller *et al.* (2020) used spinning disc reactor (SDR) with the aim of intensified (mass) nano-ZnO production. They aim to prepare needle shape zinc oxide nanoparticles. At nanoscale with this shape, the particles of Zn oxide display their maximum ultraviolet absorbance and photocatalytic activity. Average dimension of approximately 56nm was obtained after operating at different conditions, such as at different disk rotational velocity, initial concentration of Zn precursor and base solution, inlet reagent flow rate and inlet distance from disk center. The spinning disk reactor allows a uninterrupted production of nanoparticles with a capacity of 57 kg/d, with initial precursor concentration of 0.5 M and inlet flow rate of 1 L/minute . In the long run, the spinning disk rector found appropriate as a process-intensified equipment for ZnO nanoparticles synthesis.

2.2.2 Chemical Methods

Heidi van den *et al.* (2006) reviewed water based chemical routes of synthesizing zinc nanoparticles, alternative to conventional processing and gas phase synthesis. Sodium bis (2-ethylhexyl) sulfosuccinate, heptane and zinc chloride were mix to prepare an emulsion at 70°C to produce ZnO nanoparticles. PCS analysis of the emulsion represents ZnO particles of approximately 12nm in the core of micro-emulsion. A novel method for the synthesis of zinc oxide nanoparticles using ethanol-in-oil microemulsion with Zn-DEHSS (diethylhexyl sulfosuccinate) as surfactant. The microemulsion consist of Zn-DEHSS as surfactant, isooctane as continuous phase and

dry ethanol as dispersive phase. The Nanoparticles obtained were in the range of 10-13nm.

Zinc oxide nanoparticles of spherical shape with 3 to 4 nm size have been prepared by **Vafaee *et al.* (2006).** They employed TEA (triethanolamine) as surfactant for the preparation of ZnO nanoparticles. Different concentration of zinc acetate dihydrate, as precursor was used to prepare ZnO sols. Furthermore, pre-synthesized solution of ethanol and triethanolamine was mixed with the zinc acetate dihydrate solution and was stirred for 30 min. at 60°C. The novel sol-gel method represent the best optical properties can be obtain at 0.5M concentration of zinc acetate dihydrate.

Xiuping Jiang *et al.* (2010) synthesize rod-like ZnO particles employing sol-gel method. They mixed ethylene diamine (EDA) to the reaction system of $Zn(Ac)_2.2H_2O$ and $H_2C_2O_4.2H_2O$. The length and diameter of nanoparticles were about 0.2-1.5 micrometer and 20-200nm respectively, when observed using XRD and TEM. Experimental results also proved that the morphology of the zinc oxide nanoparticles can be controlled by regulating the quantities of EDA, which also plays a crucial role in the synthesis of rod-like structure. The XRD spectra of zinc oxide particles with EDA shows different peaks, assign to those of standard hexagonal phase ZnO. No separate peak of impurities were observed.

Skapin *et al.* (2009) prepared nanosized zinc oxide particles using simple precipitation method. First, hydrozincite was prepared by adding Na_2CO_3 solution and ethanol with different concentration to zinc acetate precursor. They observed, for hydrolysis the initial concentration of precursor and water used, influence the zinc of hydrozincite particles. The process of formation of ZnO nanoparticle commence at 200°C and particles of 20-50 nm were obtained at around 600°C, without agglomeration. At around 300-600°C, more pronounced XRD peaks represents the formation of ZnO nanoparticles.

2.2.3 Biological Methods

2.2.3.1 Bacterial Mediated

Bio-synthesis experiment of zinc oxide nanoparticles using bacteria *Bacillus licheniformis* MTCC 9555 and its photocatalytic activity was performed by

Tripathi *et al.* (2014). Agglomeration of zinc oxide nanoparticles was found in the form of ZnO nanorods. Further, the EDX showed the presence of elemental Zinc and Oxygen. XRD analysis represented the hexagonal wurtzite structure and crystalline nature of ZnO nanoparticles. Electron microscopy proved the it had three dimensional appearance with a range of 200-300 nm. Possible reaction mechanism behind the synthesis of nanoparticle was –

$$Zn(O_2CCH_3)_2(H_2O)_2 \rightarrow Zn(O_2CCH_3)_2$$

$$Zn(O_2CCH_3)_3 \rightarrow Zn^{2+} + 2[O_2CCH_3]^-$$

$$Zn^{2+} + 2OH^- \rightarrow Zn(OH)_2 \rightarrow ZnO + H_2O$$

Binoj nair *et al.* (2002) extracted the lactobacillus species to prepare the Coalescence of different elements in order to form submicron crystallite structure. The lactobacillus was extracted from buttermilk, after curdling it at 27°C for 24 hrs. In the filtrate that contained lactobacillus, 5mg of $AuCl_4.3H_2O$ and 1mg of $AgNO_3$ was added and left for 24hrs. First the solution turned light blue and then after 2 days it turned pale brown. Later sodium citrate was added to it, and further heated at 200°C. Citrate covered nanoparticles were prepared, with diameter 20-30 um. The smallest particle observed are in the range of 15nm and largest around 500nm.

2.2.3.2 Fungi Mediated

The study by **Arya rajan *et al.* (2016)** reports the synthesis of zinc oxide nanoparticles employing fungus *Aspergillus fumigatus*. 10 ml of 1 mM zinc sulphate, as precursor was added to the 10 ml of filtrate containing aspergillus. The solution was incubated in orbital shaker under 150 rpm at 32°C and 6.5 pH, for 72 hrs. White precipitation was collected and centrifuged at 10,000 rpm for 10 min. and lyophilized. Peak absorption was observed at 240- 385 nm by UV spectrometer and the spherical shape nanoparticles with avg. size 60-80 nm was observed under scanning electron microscope (SEM).

2.2.3.3 Algae Mediated

Susan azizi *et al.* (2013) used one pot method to synthesize zinc nanoparticles using the brown marine macroalgae, *Sargassum muticum*. 2 gm (in 100mL) of heated

and filtered dried algae powder was mixed with 2 mM zinc acetate dehydrate to prepare a solution, which was further agitated for 4 hrs. at 70°C. The pale white principate obtained was then centrifuged at 4000rpm and dried at 100°C, overnight using oven. The size of the nanoparticles were found to be around 42nm and maximum absorption was observed at 334nm. The involvement of sulfate and hydroxyl moieties of polysaccharide was revealed to be involve in the formation of ZnO nanoparticles by FTIR spectra.

In an experiment by **Sangeeta Nagarajan *et al.* (2013)** green, red and brown algae i.e. *Caulerpa peltata, Hypnea valencia and Sargassum myriocystum*, respectively, were used in the synthesis of zinc oxide nanoparticles. All these sea weeds were collected from gulf of mannar. The average size of the nanoparticles obtained were in the range of 36nm. Effect of concentration, effects of seaweed filtrate concentration, effect of temperature and effect of pH was observed. Following were the observations –

1. By increasing the concentration of zinc nitrate, increase in absorption peak was observed.
2. No absorption peak was observed on increasing the temperature.
3. At low pH, agglomeration of zinc nanoparticles takes place and at high pH no absorption peak is observed.
4. Absorption peak at pH 8 represents the reduction of zinc nitrate to zinc nanoparticles.

2.2.3.4 Plant Mediated

Synthesis of ZnO-NPs from *Hippophae rhamnoides* leaves extract via co-precipitation method of 20nm using XRD**.** They found that Eosin Y and Malachite green dye was photocatalyzed and degraded up to 95% and 89% respectively by using ZnO-NPs derived from leaves extract of *hippophae rhamnoides.*

Sukri *et al.* (2019) biosynthesize zinc oxide nanoparticles (ZnO-NPs) using *Punica granatum* (pomegranate) fruit peel extract at four different temperature. Mostly spherical and hexagonal shape ZnO-NPs were obtained in the mean size of 32.9 nm and 81.84 nm at 600°C and 700°C respectively. Also they found that smaller size ZnO-NPs were more effective in cytotoxic assay at concentration ≥31.25 ug/ml.

A Review documented by **Agarwal *et al.* (2018)** is a comprehensive study of synthesis and characterization methods used for green synthesis of ZnO-NPs using different bioproducts. Green synthesis of ZnO-NPs is employed using bacteria, plants, fungus, algae etc. ZnO-NPs had been in recent studies because of its large band gap and high exciton binding energy. **Table 2.1** represents the different plant parts used to synthesized zinc oxide nanoparticles, along with the size and the instruments used.

Photocatalytic activity of zinc oxide nanoparticles (ZnO-NPs) through green synthesis using different fruit peel extracts of *Lycopersicon esculentum* (tomato), *citrus sinensis* (orange), *citrus paradisi (grape fruit), citrus aurantifolia (lemon)* as reducing agents was performed by **Nava *et al.* (2017)**. They reported that the Surface morphology of the nanoparticle varies in shapes and sizes due to different chemical composition of fruit extract. Also, The photocatalytic activity of ZnO nanoparticles aided with UV-light exhibited maximum degradation (97%) of dye within 180 min..

Synthesis of ZnO-NPs using sol-gel approach capped with EDTA, citric acid and oleic acid was also performed to study photocatalytic activity and the kinetics of degradation of malachite green dye. EDTA capped ZnO-NPs reported to be of rod shaped and the smallest of size 29nm. Under sunlight EDTA capped ZnO-NPs showed better discoloration of dye. EDTA reported to be the best capping agent among three for the ZnO-NPs by **Meena *et al.* (2018).** In an another research **Shanker *et al.* (2017)** have reviewed the uses of ZnO, TiO_2 and Fe nanoparticles to remove dye pollution from waste water and compare their applications through adsorption and degradation method. Among dye removal techniques, adsorption was found most effective and cheap.

Table 2.1: Different plants and their parts employed in ZnO-NPs synthesis.

S.NO.	PLANT NAME	PART USED	NPs	AVG. SIZE (nm)	REFERENCE
01.	*Azadirachta indica*	Fresh leaves	Zn	18 (XRD)	**Elumalai *et al.* (2015)**
02.	*Aloe vera*	Leaf extract	Zn	8-20 (XRD)	**Ali *et al.* (2016)**
03.	*Trifolium pratense*	Flower	Zn	60-70 (XRD)	**Dobrucka *et al.* (2016)**
04.	*Rosa canina*	Fruit extract	Zn	13-25 (DLS & XRD)	**Jafarirad *et al.* (2016)**
05.	*E. crassipes*	Leaf extract	Zn	32-36 (SEM & TEM)	**Vanathi *et al.* (2014)**
06.	*Ocimum basilicum*	Leaf extract	Zn	50 (TEM & EDS)	**Abdul Salam *et al.* (2014)**
07.	*Anisochilus carnosus*	Leaf extract	Zn	20-40 (FE-SEM)	**Anbuvannan *et al.* (2015)**
08.	*Cocus nucifera*	Coconut water	Zn	20-80 (TEM)	**Krupa *et al.* (2015)**
09.	*Gossypium*	Cellulosic fiber	Zn	13 (XRD	**Aladpoosh *et al.* (2015)**
10.	*Moringa oleifera*	Leaf	Zn	24 (XRD)	**Elumalai *et al.* (2015)**
11.	*Parthenium hysterophorus L.*	Leaf extract	Zn	22-35 (XRD & TEM)	**Vafaee *et al.* (2016)**
12.	*Plectranthus amboinicus*	Leaf extract	Zn	50-180 (SEM)	**Rajiv *et al.* (2013)**
13.	*Vitex negundo*	Leaf	Zn	75-80 (SEM & EDX)	**Fu *et al.* (2015)**
14.	*Vitex negundo*	Flower	Zn	70-130 (XRD)	**Ambika *et al.* (2015)**
15.	*Nephelium lappaceum*	Fruit peel	Zn	50 (XRD)	**Sundrarajan *et al.* (2015)**
16.	*Calatropis gigantea*	Fresh leaves	Zn	30-35 (SEM)	**Yuvakkumar *et al.* (2015)**
17.	*Sphathodea campanulata*	Leaf extract	Zn	30-50 (TEM)	**Tripathi *et al.* (2015)**
18.	Solanum nigrum	Leaf extract	Zn	20-30 (XRD)	**Rames *et al.* (2015)**
19.	Phyllanthus niruri	Leaf extract	Zn	25 (FE-SEM)	**Anbuvannan *et al.* (2015)**
20.	Agathosma betulina	Dry leaves	Zn	12-26 (TEM)	**Thema *et al.* (2015)**

Production of multifunctional zinc oxide nanoparticles for dye and antimicrobial treatment in waste water was conducted by **Rambabu *et al.* (2021).** *Phoenix dactylifera* (Date palm) waste was used as bio-reductant to synthesize ZnO-NPs of diameter 30nm. DSC/TG analysis displayed the thermal stability of ZnO-NPs with <10% wt.% loss up to 700°C. Rapid decomposition rate with 90% degradation efficiency was observed against Eosin Yellow and Methylene Blue dye.

Fabrication of zinc oxide nanoparticles through green synthesis strategy using *Abelmoschus esculentus* (okra) mucilage was documented by **Prasad *et al.* (2019)** for cationic dye degradation. Hexagonal wurtzite structure of ZnO was confirmed by XRD with avg. size of 29nm, elongated and rod like structure. Selective photodegradation of targeted dye was observed, where 125mg of the ZnO-NPs removed 100% of the Methylene Blue solution (32mg/L) within 60min. and 100mg of ZnO-NPs was needed in removal of Rhodamine B (9.5mg/L) within 50min.. Photodegradation was confirmed by liquid chromatography- mass spectrometry analysis.

Mallikarjunaswamy *et al.* (2019) reported the synthesis of ZnO-NPs by microwave irradiation method using *Aegle marmelos* (Indian bale) juice as fuel. Also, the degradation of Methylenenblue was observed using above synthesized nanoparticles. Photoluminescence spectrum showed the excitation wavelength of 370nm and emission peak at 388nm and 468nm corresponding to Zn vacancies and 0 vacancies respectively. After 35 min. of UV (λ-617nm) irradiation, the dye degradation efficiency was found to be 96%.

Iron oxide nanoparticles modified with tangerine peel extract (Ti-Fe_3O_4) were also utilized to carry batch adsorption experiment for the removal of lead from aqueous solution**.** They observed 99% removal of Pb^{+2} with 0.6 g/l of Ti-Fe_3O_4 at an initial concentration of Pb at 10 ppm. Also, the adsorption isotherm was found to be monolayer on the homogenous surface of the adsorbent. Besides, **El-Gendy *et al.* (2019)** also reviewed that Nano-biocides of biological origin such as metal nanoparticles proved to be marvellous waste water treatment agents and have various opportunities and limitation in removal of contaminants.

Sharma *et al.* (2018) reported the different biomolecules that are present in plants and can be utilized in the synthesis of nanoparticles. They reported, plant extracts possess a combination of biomolecules including amino acids, proteins, enzymes, alkaloids, polysaccharides, saponins, tannins, terpenoids, phenolics, vitamins, and flavonoids, that can be incorporated during nanoparticle synthesis. These biomolecules are also capable of chelating and reducing metal ions to their nanoparticle state. **Table 2.2** represents the list of different biomolecules that can be used in synthesis of nanoparticles.

Various fruit peel extracts were utilised as reducing agents to convert zinc nitrate, which was used as a source of zinc ions, to its nanoparticle state **(Nava *et al.*, 2017).** The peels of *Citrus aurantifolia* (lemon) and *Citrus paradisi* (grapefruit) were heated to physiologically manufacture ZnO NPs. Presence of flavonoids, carotenoids, and limonoids functioned as reducing agents. Band at 618cm^{-1} was observed in all samples, suggesting the presence of the Zn-O bond. In structure, all samples showed the identical hexagonal crystal development. UV light aided methylene blue degradation was used to examine the zinc oxide nanoparticles photocatalytic capabilities. When compared to chemically manufactured commercially available zinc oxide nanoparticles, most samples showed a disintegration rate of roughly 97% after 180 minutes.

The biogenesis of ZnO NPs was reported by **Chaudhuri and Malodia, (2017)** using *Calotropis gigantean* leaf hot water extract. The interaction of 15 ml of leaf extract with 200 mM zinc acetate salt resulted in the formation of ZnO NPs with a diameter of 20nm. At roughly 350nm, an absorption band developed that is unique to ZnO-NPs. The polydispersity index (PdI) of the DLS data was 0.245, with a single peak at 11nm (100 percent). They were highly crystalline, with an average size of 10 nm, according to the XRD examination. EDX revealed the presence of oxygen and zinc, with atomic percentages of 68.69 and 33.31, respectively. AFM experiments yielded two-dimensional (2D) and three-dimensional (3D) pictures of ZnO-NPs, revealing that they were monodispersed with size ranges between 1.5 and 8.5 nm. The production of ZnO-NPs was facilitated by the presence of phytochemicals, flavonoids, and volatile essential oils.

The work by **Jamkhande *et al.* (2019)** intended to biosynthesize zinc oxide nanoparticles (ZnO NPs) via facile and modern route using aqueous *Ziziphus jujuba* leaves extract assisted by microwave and explore their photocatalytic degradation of methyl orange (anionic dye) and methylene blue (cationic dye) under solar irradiation. The biosynthesized microwave assisted ZnO-NPs were characterized and the results showed well-defined spherical-like shape with an outstanding band gap (2.70 eV), average particle size of 25nm and specific surface area of 11.4 m^2/g. Under solar irradiation, the photocatalytic degradation of the MO and MB dyes by biosynthesized ZnO NPs was investigated, and the results demonstrated the ZnO-NP's selective character for the adsorption and subsequent photocatalytic destruction of the MO dye compared to the MB dye.

Table 2.2: Biomolecules used in the synthesis of nanoparticles.

Class of compounds	***Examples***	***Chemical structure***	***Type of NPs produced***
Polysaccharides	Alginic acid	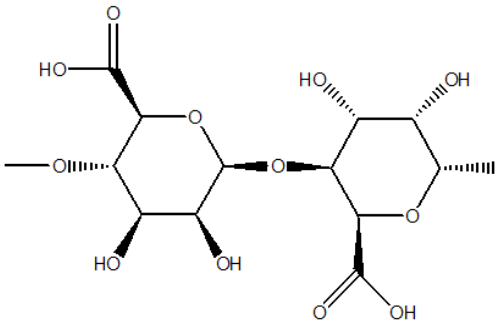	Zinc oxide NPs
Vitamins	Ascorbic acid	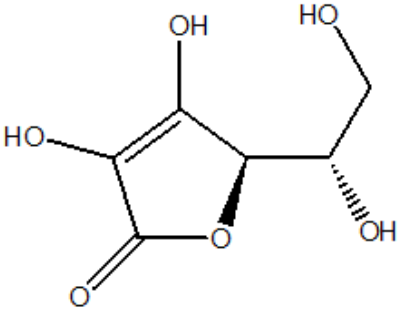	Zinc oxide NPs

Sugar alcohol	Mannitol	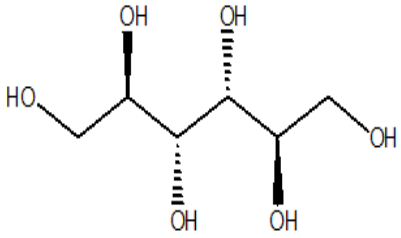	Zinc oxide NPs
Sugar derivatives	2,3-Dihydro-3,5-dihydroxy-6-methyl-4H-pyran-4-one (DDMP)	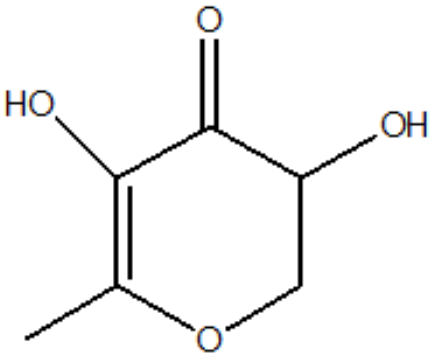	Iron oxide NPs
Flavonoids	Kaempferol	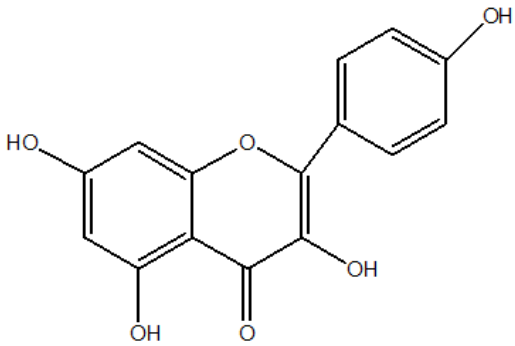	Zinc oxide NPs
Flavonoids	Hesperitin	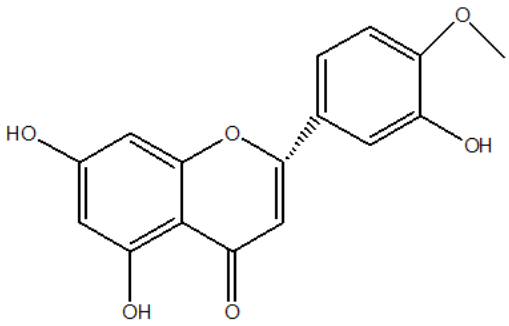	Zinc oxide NPs

Flavonoids	Quercitrin	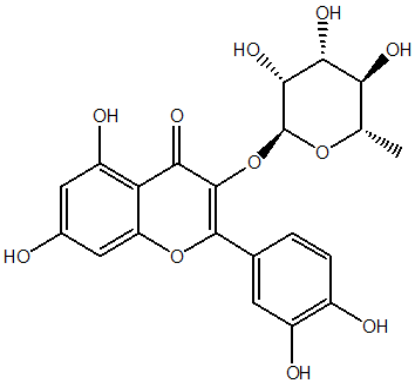	Zinc oxide and titanium dioxide NPs
Phytosterols	Sitosterol	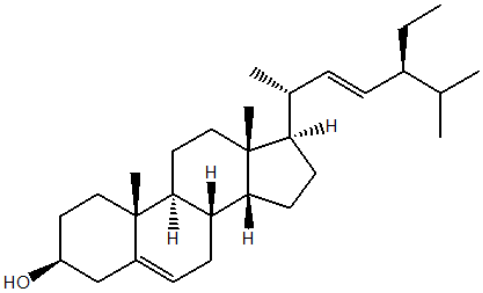	Zinc oxide NPs
Phytosterols	stigmasterol	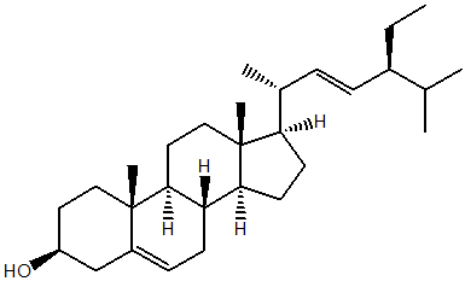	Zinc oxide NPs
Glucose derivatives	Glucoside	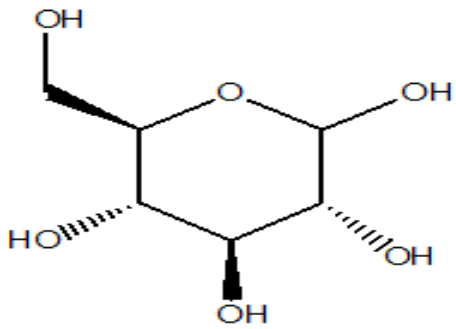	Zinc oxide NPs
Furano-flavonoids	Karanjin	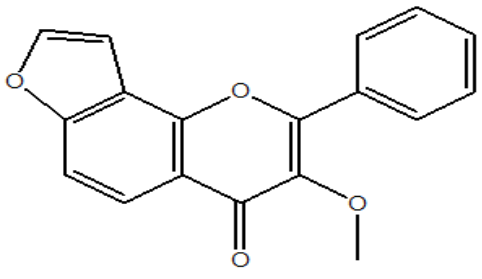	Zinc oxide NPs

	Pongamol	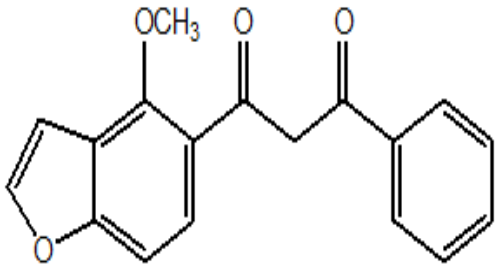	
	Pongapin	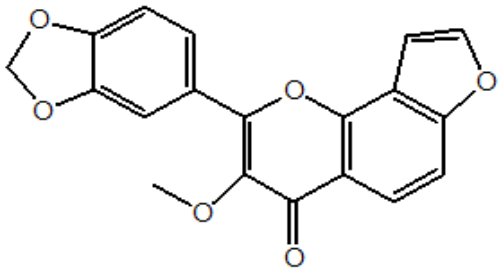	
	Pongaglabrone	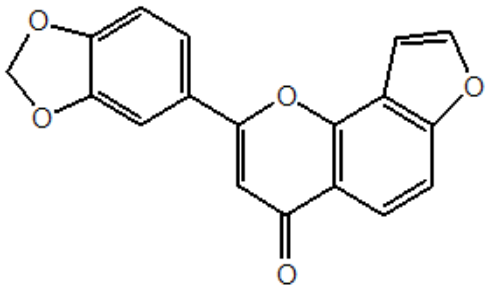	
Phenolic compounds	2-methylanthraquinone	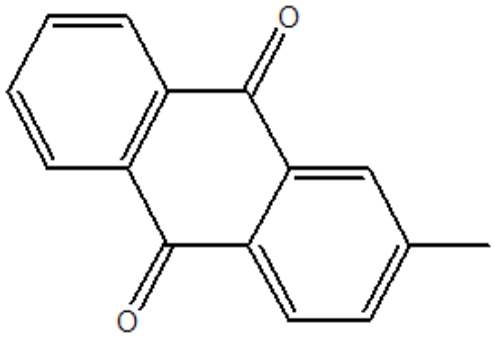	Zinc oxide NPs

Romelle *et al.* (2016) performed an experiment on selected fruit peels to investigate their chemical composition. Peels of fresh fruits (pineapple, apple, mango, pomegranate, banana) were removed and examined for their nutrients and anti-nutrients contents. The lipids, proteins, ash, crude fibre and carbohydrates content in fruit peels were respectively from 3.36 ± 0.37 to 12.61 ± 0.63%, from 2.80 ± 0.17 to 18.96 ± 0.92%, from 1.39 ± 0.14 to 12.45 ± 0.38%, from 11.81 ± 0.06 to 26.31 ± 0.01% and from 32.16 ± 1.22 to 63.80 ± 0.16%. The phenolic contents of fruit peels

ranged from 0.91 ± 0.06 to 24.06 ± 0.89%. Oxalates, hydrogen cyanide, phytates and alkaloids levels in fruit peels were also within threshold safe limit. **Table 2.3** shows the alkaloids, phytates and phenolic contents of sampled fruit peel waste.

Table 2.3: Percentage level of Reducing agents in different fruits peel.

Fruit peels	Alkaloids content (%)	Phytates content (%)	Total phenolics content (%)
Pineapple	16.19 ± 3.28	1.99 ± 0.01	1.42 ± 0.09
Mango	8.34 ± 1.21	1.63 ± 0.10	24.06 ± 0.89
Apple	7.99 ± 1.19	1.42 ± 0.20	8.86 ± 0.09
Banana	6.88 ± 0.78	6.02 ± 0.61	7.40 ± 0.17
Orange	5.44 ± 0.72	2.34 ± 0.47	13.54 ± 0.96
Pomegranate	6.50 ± 0.62	1.33 ± 0.10	22.67 ± 0.27
Watermelon	10.09 ± 1.78	0.70 ± 0.17	0.91 ± 0.06

Values are means ± standard deviations of three replicate measurements.

Materials and Methods

Chapter 3 MATERIALS AND METHODS

The experiment was conducted at the Department of environmental sciences, college of basic sciences and humanities, G.B. Pant University of Agriculture and Technology in the month of April-May with the avg. room temperature of 32°C. The GPS coordinates are, 29.0229°N 79.4879°E and the elevation is 243.84m (800ft) above sea level which is considered as Tarai region of Uttarakhand. This chapter is about the material used and the procedure adopted, to fulfil the goals of present investigation. This includes biosynthesis, characterization and photocatalytic activity of zinc oxide nanoparticles derived from mixed fruit peel waste.

3.1 Chemicals and Reagents

Zinc nitrate hexahydrate was obtained from sigma Aldrich chemicals (analytical grade), ethanol was procured from Hi-media laboratories India, sodium hydroxide was taken from Hi- media laboratories India, and Malachite green from SRL chemicals India.

3.2 Plastic Wares and Glass Wares

The glass wares used during the study were procured from Borosil, India Ltd. The plastic wares were supplied by Tarson, India and Polylab, India.

3.3 Instruments Used

Table 3.1: List of Instruments

Name of Instruments	Manufacturer
Double beam UV-Vis Spectrophotometer	Model 5704 – ECI Hyderabad, India
pH meter	Model L1 -120 – Elico India Ltd., New Delhi.
Digital balance	Model AD-60 B - Adair Dutt and Company, New Delhi.
Grinder (I.H.P.)	Scientronic Instruments, New Delhi.
Hot air oven Universal	Indian Equipment Corporation, India.
Refrigerator	BPL Ltd., India
Centrifuge	Neuation Technologies Pvt. Ltd
Muffle furnace	Biological Enterprises
Hot plate	Marco Scientific Work, New Delhi

3.4 Collection of mixed fruits peel waste

All the fruits (apple, grapes, oranges, banana and pomegranate) were collected from nearest supermarket, G.B. Pant University of Agriculture and Technology, Pantnagar, Uttarakhand.

3.5 Preparation of mixed fruits peel extract

Fresh fruits were collected and washed thoroughly, first with tap water and then with distilled water to clean the dust particles or any kind of impurities. After this, fruits were carefully peeled, as thin as possible, using kitchen knife and then further chopped into small pieces. 100gm of each chopped fruit peels were weighted carefully and then mixed. The mixed chopped fruit peels were then oven dried at 60°C for 36hrs **(figure 3.1)**. Dried fruits peels were grounded into fine powder using electrical mixer grinder. For the preparation of leaf extract, 20gm of mixed fruit peel powder was dissolved in 100ml of distilled at room temperature in beaker using glass rod. This mixture was then transferred to conical flask for autoclave. The mixture was autoclaved at 121°C temperature and 15 pounds per square inch pressure for 30min., to eliminate any kind of contamination. After autoclaving the extract for desired duration, it was flirted using a normal size mesh to remove all the undissolved chunks of peel powder **(figure 3.2).** The obtained extract was then centrifuged at 8000rpm for 10min. to remove the colloidal particles and the finally filtered using what man no. 1 to get pure extract. After several layer of filtration, 40ml of stock mixed fruit peel extract was obtained, which was then stored at 4°C for further experiment.

3.6 Biogenic synthesis of zinc oxide nanoparticles

Zinc nitrate hexahydrate [$Zn(NO_3)_2.6H_2O$] was used as the precursor compound for Zn nanoparticles synthesis. Its stock solution was prepared by dissolving 1.25gm of zinc nitrate hexahydrate in 100ml distilled water. To regulate the pH of the nanoparticle synthesis reaction, 0.2M stock solution of sodium hydroxide was also prepared.

20ml of fruit peel extract was added to 80ml of zinc nitrate hexahydrate solution with continuous stirring. The obtained solution had light brown colour

(figure 3.3). This solution was then transferred to preheated (70°C) hot plate with magnetic stirring 500rpm, by magnetic stirrer. Sodium hydroxide was added dropwise with continuous stirring, after the solution kept over hot plate got little warmed.

Collect fresh fruits

↓

Wash the fruits with distilled water

↓

Peel the fruits as thin as possible

↓

Oven dry it at 60°C for 36hrs

↓

Ground the peel into fine powder using electrical grinder

↓

Add 20gm of mixed fruit peel powder into 100ml of water

↓

Autoclave it for 30mins. at 121°C temp. and 15psi pressure

↓

Filter the solution using normal mesh to remove large particles

↓

Centrifuge the solution at 8000rpm for 10min.

↓

Filter again using Whatman no. 1

↓

Store the filtrate at 4°C

Figure 3.1: Process flow chart for preparation of mixed fruit peel extract.

(a)

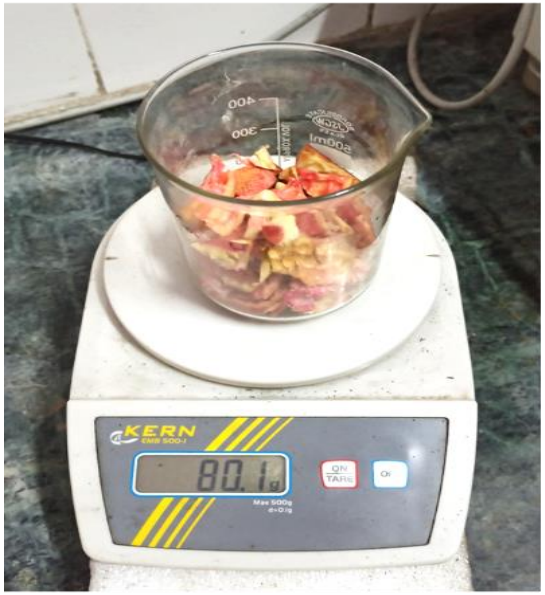

(b)

(c)

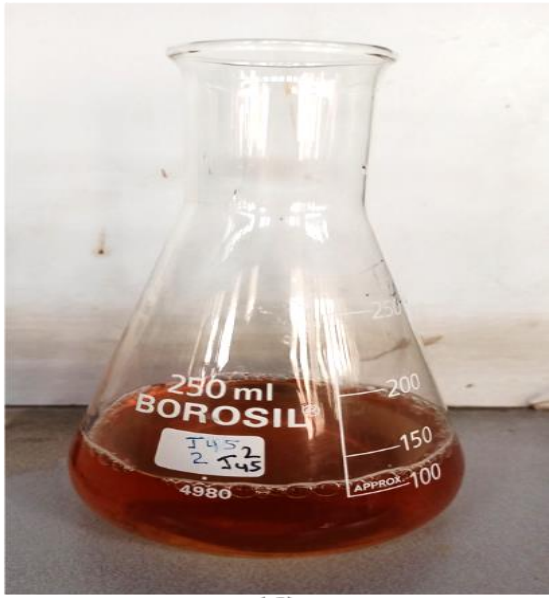

(d)

Figure 3.2: Fruits peel extract preparation (a) collection of peels, (b) weighing of peels, (c) weighing of peel powder and (d) collection of fruits peel extract

The solution was continuously stirred for 2hr. After 2hr the initial brown colour solution was changed to pale yellow with white precipitation. The formation of white precipitation represents the formation of nanoparticles. After bringing the pale yellow colour solution to room temperature, it was transferred to test tube and centrifuged at 8000rpm for 15min., twice. The fine white precipitation was collected into petri dish using ethanol and spatula. The procured white colour precipitate was then oven heated at 60°C for 12hrs. to carry the conversion of $Zn(OH)_2$ to zinc oxide nanoparticles. Next day, the obtained white colour precipitate was transferred to glass vials and stored at 25°C for further studies **(figure 3.4).**

3.7 Photocatalytic activity of zinc oxide nanoparticles

3.7.1 Effect of ZnO NPs loading

The efficiency of biosynthesized ZnO NPs was assessed by its capacity to degrade malachite green dye. A 20ppm stock solution of malachite green was prepared by dissolving 20mg of malachite green to 1000ml. Different concentrations of ZnO NPs, i.e. 50ppm, 100ppm, 150 ppm, 250ppm were mixed with malachite green solution. The mixture was then agitated to obtain adsorption equilibrium. After mixing, the solutions were transferred to direct sunlight. At specific time intervals, small samples were measured against absorbance to evaluate the photocatalytic degradation of dye. The catalytic activity was continued for 0, 50, 100, 150, 200, 250 minutes. Later, the graphs and the degradation percentages was calculated using obtained absorbance value, to estimate the effectiveness of ZnO NPs.

Percentage (%) degradation of dye was calculated by the given formula:

$$\textbf{\% Degradation} = [\ (A_\circ - A)/A_\circ\ ] \times 100$$

Where,

$A_\circ$ = Initial absorbance

A = Absorbance of dye after photocatalytic degradation.

3.7.2 Effect of dye concentration

After performing the catalyst loading experiment, the best catalyst load was picked and added to different concentrations of dye. The zinc oxide nanoparticles were added to 10, 15, 20, 25, 50, 100ppm concentrations of dye. After fixed intervals the absorbance of the samples were measured. Graphs and the degradation percentages were calculated using obtained absorbance value, to estimate the effectiveness of ZnO NPs at different dye concentration.

Selection of precursor compound for the synthesis of zinc oxide nanoparticles (zinc nitrate hexahydrate, zinc acetate etc.)

↓

Add 1.25gm of **zinc nitrate hexahydrate** to 100ml distilled water to prepare its stock solution

↓

Add 20ml of fruit peel extract to 80ml of $Zn(NO_3)_2.6H_2O$ solution

↓

Keep the mixture on pre-heated (70°C) hot plate with continuous stirring

↓

Boil the solution until the colour changes from dark green to pale yellow with white ppt. indicating the formation of zinc oxide nanoparticles

↓

Centrifuge the pale yellow solution at 8000rpm for 15mins.

↓

Collect the white precipitate after centrifuge using ethanol

↓

Oven dry the wet precipitate at 60°C for 12hrs

↓

Collect and store the zinc oxide nanoparticles at 25°C

Figure 3.3: Flow chart of the biosynthesis of zinc oxide nanoparticles from mixed fruits peel extract.

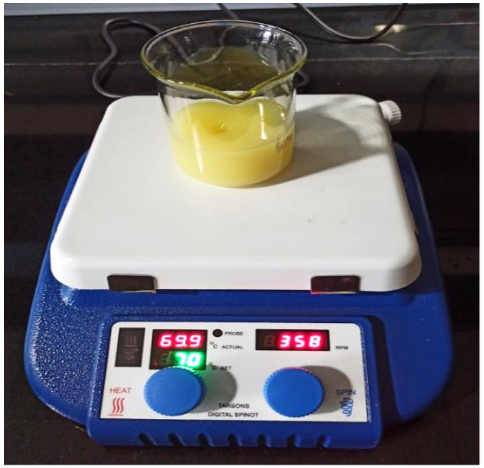

(a)

(b)

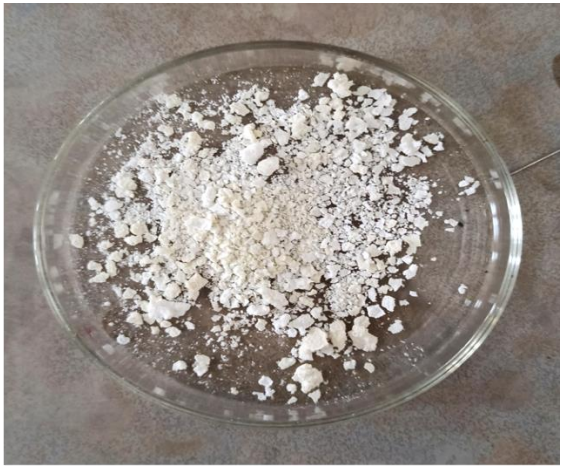

(c)

(d)

Figure 3.4: ZnO NPs preparation (a) reaction between zinc precursor and fruits peel extract, (b) wet ZnO NPs (c) oven dried ZnO NPs and (d) MG degradation experiment setup

3.7.3 Effect of pH

To evaluate the effect of pH on the degradation process, experiments at different pH were performed. The best dye and nanoparticle concentration was used from the previous experiments and the dye degradation experiments were performed again at pH 5, 7, 9 and 10. The pH of the samples were adjusted using 0.1N HCL and 0.1N NaOH, before adding the nanoparticles. The mixture was then agitated to obtain adsorption equilibrium. At specific time intervals, small samples were measured against absorbance to evaluate the photocatalytic degradation of dye. Observations were recorded after 0, 15, 30, 45, 60mins. The graphs and the degradation percentages was calculated using obtained absorbance value, to estimate the effectiveness of ZnO-NPs in degrading MG dye at different pH conditions.

3.8 Characterization Studies

3.8.1 UV- visible spectrophotometer

UV-vis spectroscopy was used to validate, the generation of metal oxide nanoparticles by green synthesis and photodegradation of malachite green employing the zinc oxide nanoparticles. The presence of nanoparticles was indicated by the presence of an absorbance peak in the region of 300-700nm. The experiment was carried out using an Ultrospec 2100 pro with a cuvette length of 10nm.

3.8.2 Dynamic light scattering (DLS) analysis

The DLS technique is used to estimate the hydrodynamic diameter of nanoparticles. It calculates the Z-average (d.nm.) and PDI value of nanoparticles at a constant temperature of 25°C. As a reference, we utilised the refractive index of 1.3328, the dielectric constant of 78.3, and the viscosity of pure water. As dynamic light scattering is a spectroscopic measurement technique, it relies on the numerical transformation of spectral measurement data into size distributions in the sample. The basic principle of dynamic light scattering (DLS) is to detect coherent light scattered by scattering objects such as big molecules or fine particles in a time-resolved manner.

3.8.3- Fourier transform infrared (FTIR)

The functional group contained in physiologically reduced nanoparticles was identified using the FTIR. It is designed to operate between 400-4000cm^{-1} range for absorption maxima.

3.8.4 Scanning electron microscopy (SEM)

The high resolution Scanning Electron Microscope is an excellent and extensively used tool for determining shape and size since image acquisition and sample preparation are easy and quick. Furthermore, the SEM resolution technique can determine surface morphology, absolute particle size, aggregation, dispersion, crystal structure and surface functionalities. It also explains the nanoparticles shape, crystallinity, and porosity. Although the SEM picture is a two-dimensional (2D) depiction of three-dimensional (3D) objects from a specific viewing angle, it does contain a certain amount of 3D information that can be utilised to reconstruct the geometry of a simple structure with sub-nm precision using model-based measurement.

3.8.5. Energy Dispersive X-ray Spectroscopy (EDS/EDX)

EDX is used to measures the X-rays emitted by the sample. Because X-ray energy is a significant aspect of an atom's electronic structure, it can utilized to perform both qualitative and quantitative study of the sample. Elements with atomic numbers ranging from beryllium to uranium can be identified using EDX. The minimal detection limit range falls from 0.1 to a few atomic percent, depending on the sample element and EDX detector. Background signal intensities can be refined to get intensities of characteristic peak of the forming elements based on the specified sensitivity factor, which can be experimental or computed, and thus quantitative findings can be produced.

3.8.6 X-Ray Diffraction (XRD)

X-ray diffraction is used to address information related to solid crystal formations. It contain strain defects, lattice constants, material identification, geometry, stress, individual crystal orientation, average grain size in crystal structures.

In XRD, an X-ray beam is incident on the sample to be studied and is diffracted by crystalline phases according to Bragg's law. Powder diffraction patterns are recorded using a diffractometer, and relative intensities of diffraction lines and d-values are calculated to identify an unknown chemical. The acquired data is compared to the Powder Diffraction File (PDF) database, which contains typical line patterns of numerous substances. The International Centre for Diffraction Data (ICDD) updates its PDF database once a year, including about 60,000-line patterns of various crystallographic phases.

Results and Discussion

The outcomes of the experiments conducted is described in this chapter. The results of synthesis of ZnO NPs and degradation of malachite green dye were examined and outcomes are presented with the support of tables and figures. The discussions on significant experiments results obtained during the investigation have also mentioned in this chapters.

4.1 UV-Visible Spectrophotometric analysis

ZnO NPs was procured after oven drying the obtained pale white precipitate. The powder was suspended in deionized water and sonicated for 15min. to observe the UV-visible spectrum, which revealed an excitonic absorption peak around 370nm–378nm **(Figure 4.1).** The peak 378nm indicates the formation of ZnO NPs **(Nava *et al.*, 2017).** Zinc oxide's characteristic absorption peak might detected due to intrinsic band gap as excited electrons from its valance band travels to conduction band.

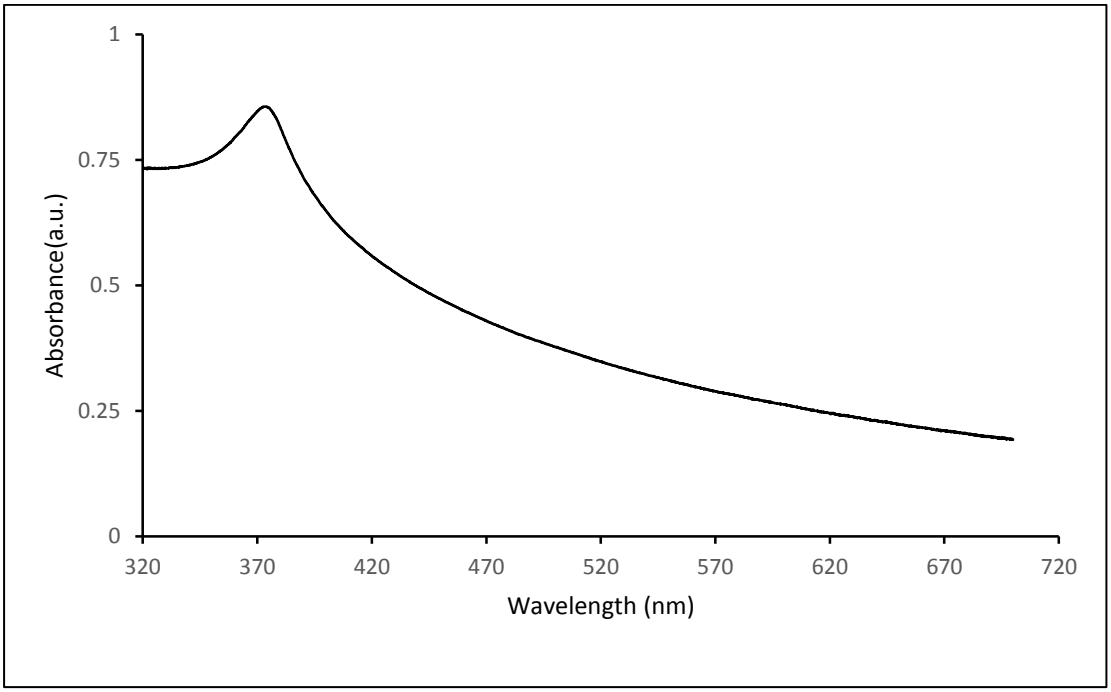

Figure 4.1: UV-Vis spectrum for ZnO NPs.

4.2 Dynamic light scattering (DLS) analysis

DLS is a new and widely used method for calculating hydrodynamic diameter of nanoparticle suspension based on the Brownian motions shown by the particles. Average hydrodynamic diameter of 162.1nm was reported through DLS analysis **(Figure 4.2)**, which is significantly bigger than the sizes reported by FE-SEM. This deviation in nanoparticle sizes could be due to their polydisperse nature. The polydispersity of nanoparticles indicates their nature. The PdI value for the sample was found to be 0.194. Polydispersity is a term used to describe the degree of "non-uniformity" in a distribution, which in the case of nanoparticle suspensions could be linked to the occurrence of nanoparticles as aggregates or agglomerates, resulting in variability in calculated particle size compared to actual particle size **(Pragati *et al.*, 2016).**

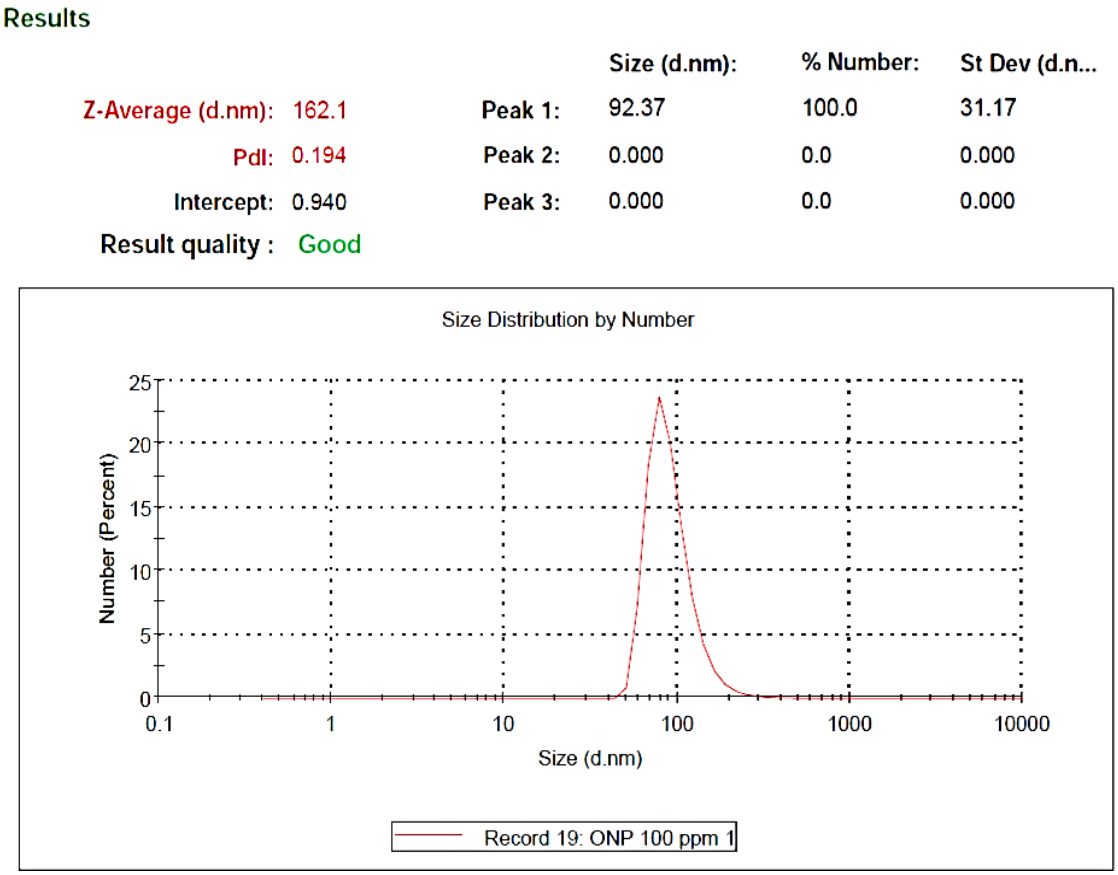

Figure 4.2: DLS report of ZnO NPs suspension.

4.3 Fourier Transform Infrared Spectroscopy (FT-IR)

The size, shape, and functionalization of ZnO NPs generated through optimization were determined using several analytical techniques. To begin, FT-IR spectroscopy was used to assess the involvement of fruit peel extract in the reduction and stabilisation of nanoparticles. FTIR spectra revealed peaks at 3589.6, 3424.02, 2375.42, 1645.95, 1456.7, 1395.15, 863.95, and 674.76cm^{-1} **(Figure 4.3).**

The peak at 3589.6cm^{-1} and 3424.02cm^{-1} represents the H bonded OH stretch and N-H stretch, respectively. The peak at 2375.42cm^{-1} corresponds to C stretching vibrations, or alkynes stretching vibrations. The stretching bands of C=O functional groups produce the 1645.95cm^{-1} peak. The amine (-NH) vibration stretch in protein amide bonds is represented by the peak at 1396.15cm^{-1}. The 863.95cm^{-1} and 674.76cm^{-1} peaks, respectively, correlate to alkanes and alkynes bends **(Yanli Gao *et al.*, 2020).**

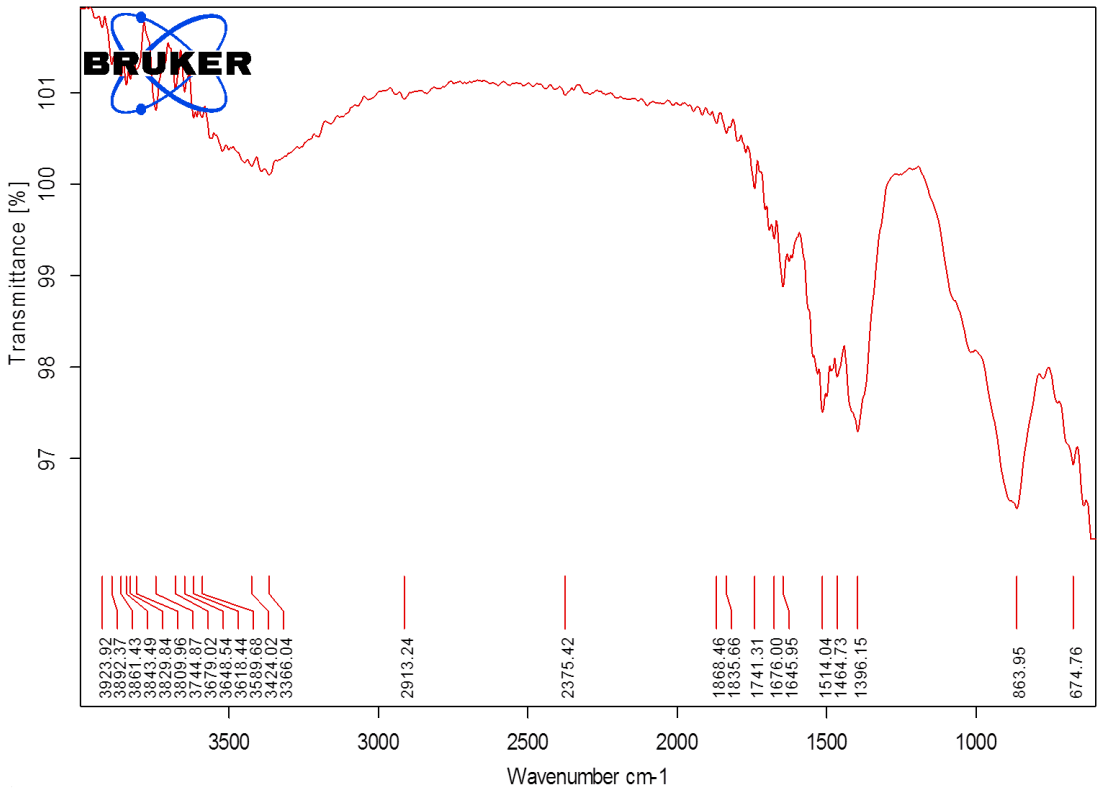

Figure 4.3: FTIR spectrum for ZnO NPs.

4.4 X-Ray Diffraction (XRD): Structural analysis

To characterized the structural properties of sample Phillips PANA lytical X'PERT PRO Diffractometer with Cu target (λ=1.5404) was used. In XRD, X-ray beam is made incident on sample to be analysed and get diffracted by crystalline phases according to Bragg‘s law. The Bragg‘s equation is given as follows:

$$n\lambda = 2\,d \sin\theta$$

Where, n is known as the order of reflection and is an integer, λ is the X-rays wavelength, θ is the angle between the incident beam and the normal to the reflecting lattice plane and d is spacing between crystal planes in the given sample. **Figure 4.4** shows the XRD patterns of synthesized ZnO NPs. Diffraction peaks were found in sample. The planes (100), (002), (101), (102), (110), (103), (200),(112), and (201) confirm the formation of pure hexagonal wurtzite phase ZnO, which agrees well with the standard ICDD card No. 01-079-0205 **(Sukri *et al.*, 2019).**

4.5 Field emission scanning electron microscopy (FE-SEM) and Energy Dispersive X- Ray Analysis (EDX)

Field emission Scanning electron microscopy (FE-SEM) images of ZnO NPs are shown in **figures 4.6a, 4.6b and 4.6(c),** respectively. As shown in **figures 4.6**, few ZnO NPs are in spherical shape and most of them are in triangular shape. At some locations agglomeration can also be seen. The size of the nanoparticles were found to be in the range of 60-100nm. The EDX spectra shown in **figure 4.5**, confirms the presence of zinc and oxygen. EDX for ZnO NPs also represents peaks for carbon and calcium. The elements C and Ca are significant nutrients in fruits peel used, and the occurrence of their peaks in ZnO NP’s EDX spectrum could have come from the extract used **(Anju devi *et al.*, 2020).**

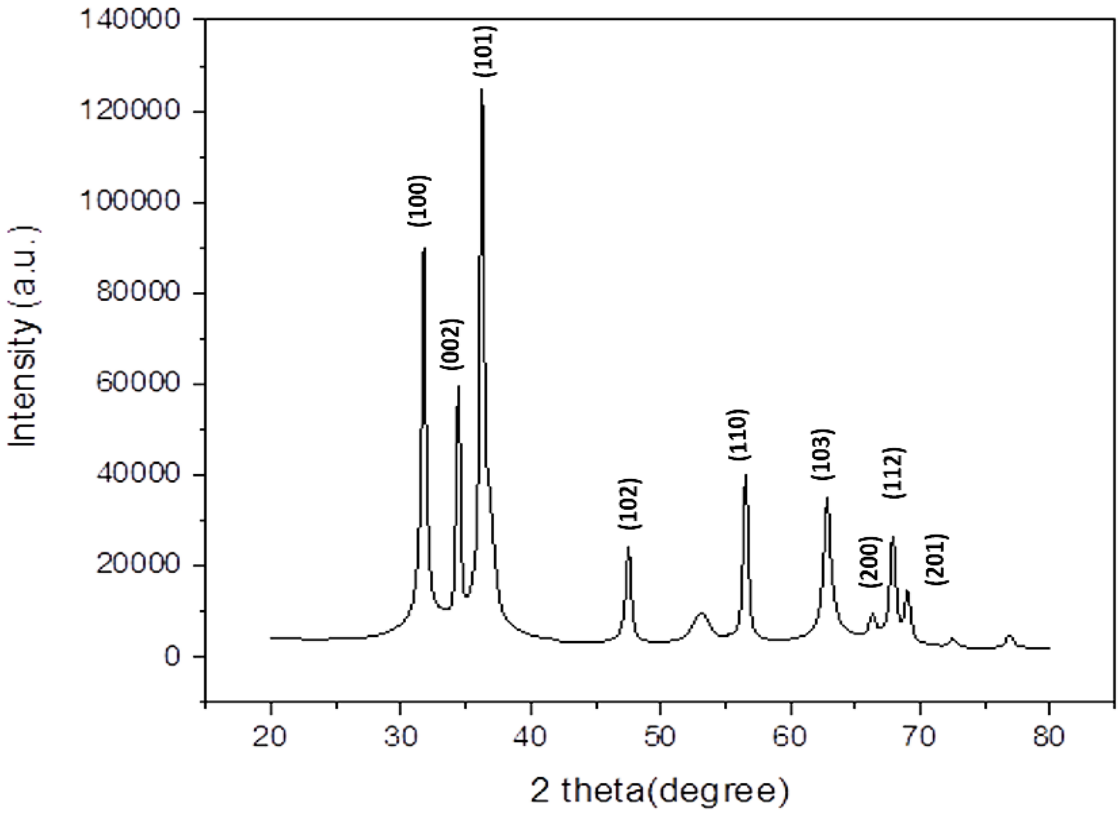

Figure 4.4: XRD spectrum for ZnO NPs.

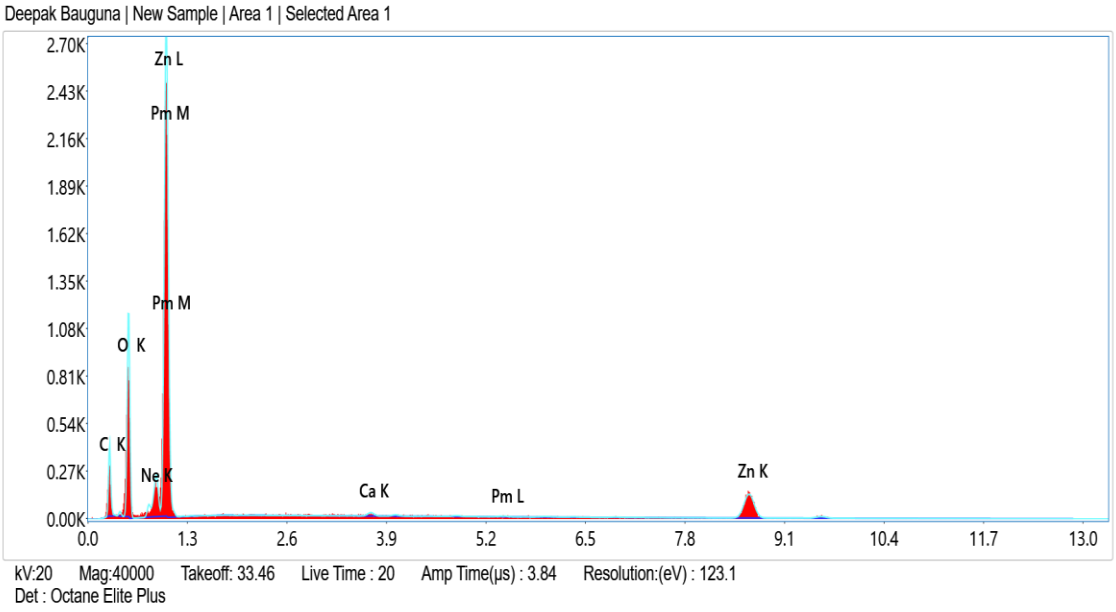

Figure 4.5: EDX spectrum for ZnO NPs.

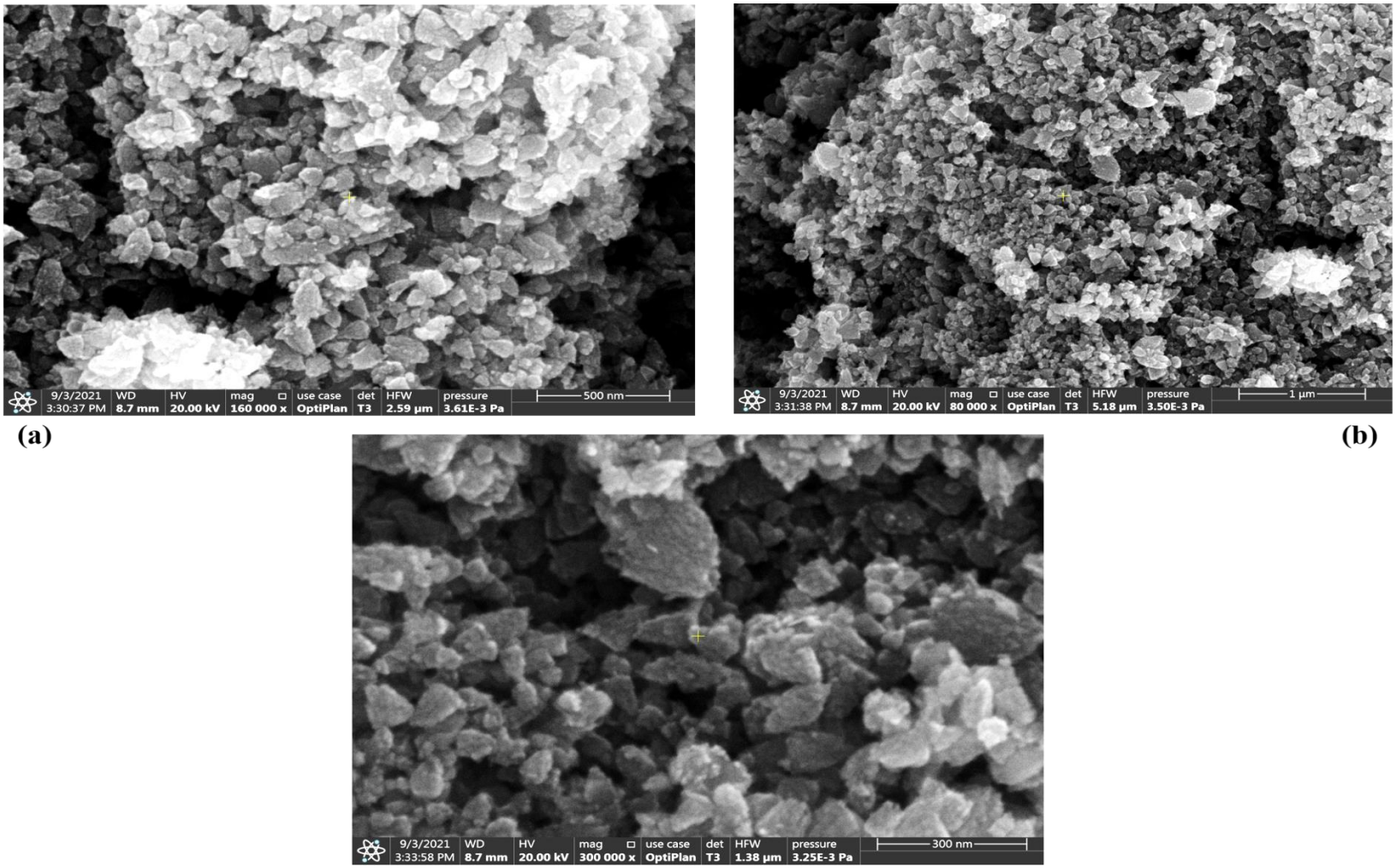

Figure 4.6: FE-SEM images of ZnO NPs at (a) 500nm, (b) 1µm and (c) 300nm scale.

4.6 Photocatalytic Study

Effect on photocatalytic activity of synthesized ZnO NPs towards the degradation of Malachite green dye was investigated at different conditions such as different initial ZnO NPs concentration, dye concentration and pH, process of which is already explained.

4.6.1 Effect of ZnO NPs concentration

Experiments were carried out with varying doses of ZnO NPs (50ppm, 100ppm, 150ppm and 250ppm) while the dye concentration and pH were kept constant at 20ppm and 7, respectively. The absorption spectra was recorded after every 50mins. of irradiation and was recorded up to 250mins. **Figure 4.7 (a)-(d)** represents the absorbance spectra of ZnO NPs dosage at 50, 100, 150 and 250ppm respectively. The line graph in **figure 4.8** displays percent degradation vs. irradiation duration and the bar graph in **figure 4.9** displays percent degradation vs. ZnO NPs concentration at different irradiation duration, and it can be shown that the degradation efficiency improves with ZnO NPs loading and declines as the ZnO NPs amount is increased. Previous studies have shown, with more nanoparticles, the availability of active sites (hydroxyl and oxygen radicals) rises, resulting in increased photocatalytic activity. However, after reaching an optimum value, high ZnO NPs dose causes agglomeration, which reduces the active sites for dye molecule adsorption. Additionally, a larger ZnO NPs concentration might also induce turbidity, which lowers light penetration due to scattering **(Anju devi *et al.*, 2020).**

Table 4.1: Percent degradation of MG dye at different ZnO NPs concentration.

Concentration	**Time**					
	0 (min.)	**50 (min.)**	**100 (min.)**	**150 (min.)**	**200 (min.)**	**250 (min.)**
50 ppm	0	8.52	21.23	33.50	42.60	63.07
100 ppm	0	19.56	32.73	51.94	67.84	83.81
150 ppm	0	**33.95**	**50.73**	**72.83**	**85.71**	**93.08**
250 ppm	0	20.36	46.02	59.12	64.04	70.47

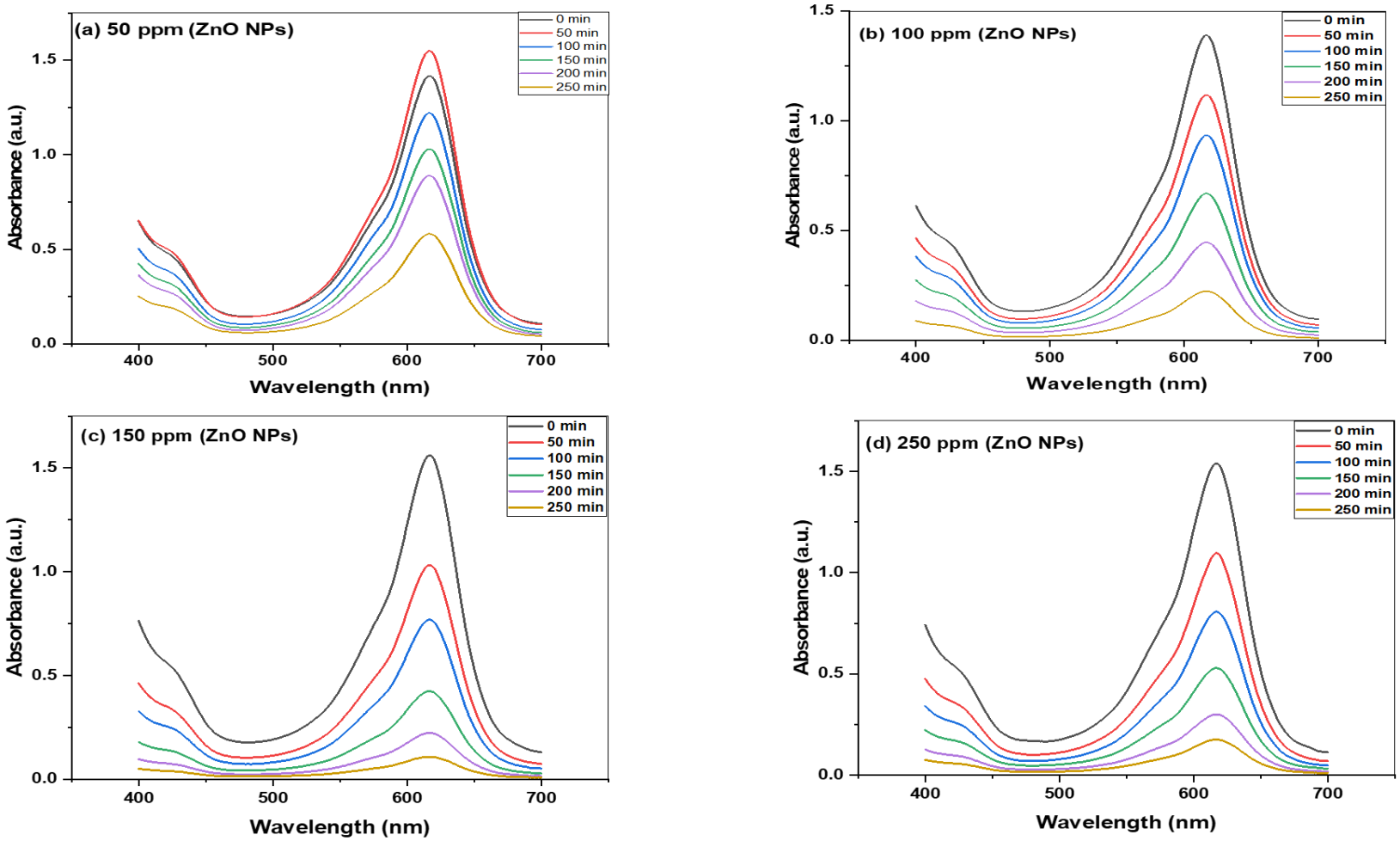

Figure 4.7: UV-Visible spectra of degradation of MG dye at different ZnO NPs concentration (a) 50ppm, (b) 100ppm, (c) 150ppm and (d) 250ppm.

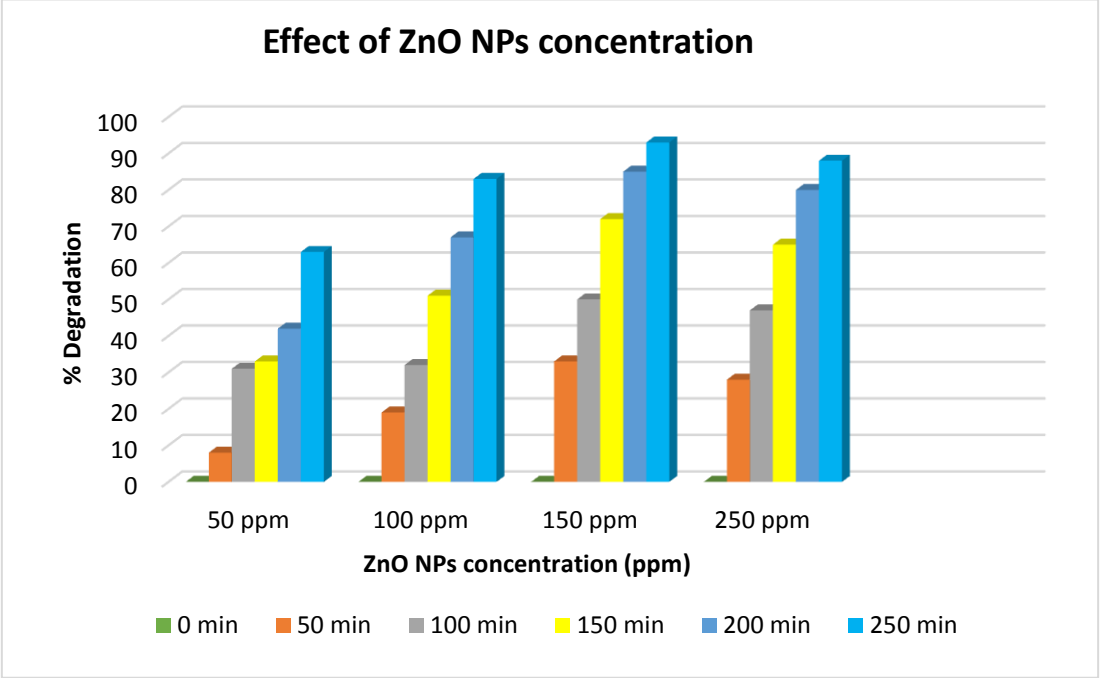

Figure 4.8: Percent degradation vs ZnO NPs concentration graph.

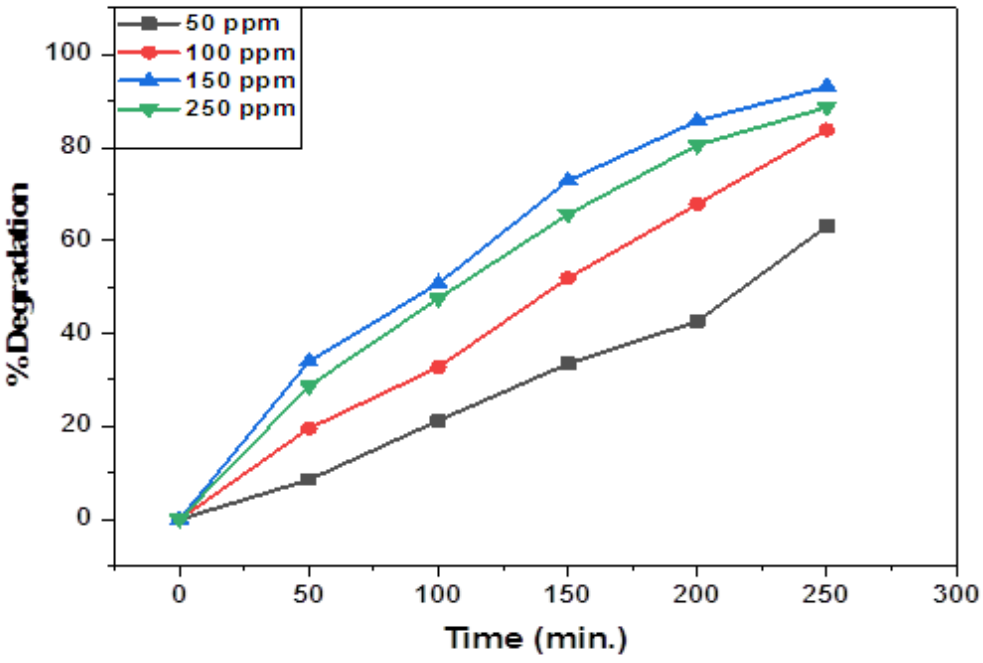

Figure 4.9: Percent degradation Vs irradiation time graph at different ZnO NPs conc.

4.6.2. Effect on dye degradation

Textile effluent of any typical industry has the dye concentration range from 0.15 to 0.2gL^{-1}. For varied dye concentrations of 10ppm, 15ppm, 20ppm, 25ppm, 50ppm and 100ppm, with fixed amount of ZnO NPs at 150ppm and pH 7, the influence of the initial dye concentration on the photocatalytic activity was investigated **(figure 4.10).** For varying initial dye concentrations, different degradation was observed, as shown in **table 4.2. Figure 4.11** depicts the percent degradation with dye concentration and irradiation time. Another **figure 4.12** represents the percentage degradation of malachite green with time, in presence of nanoparticles. The degradation efficiency was shown to improve with dye concentration and then decrease, with 20ppm yielding the best results. As the dye concentration rises, the reaction between dye molecules and catalyst becomes easier, increasing the percentage of dye breakdown. When the dye concentration reaches an optimum level, the dye molecules cover the catalyst, preventing light from entering and creating a screen effect. As a result, electron-hole formation will be reduced, and photodegradation will be reduced **(Pragati jamdagni *et al.*, 2016).**

Table 4.2: Percentage degradation of MG dye at different dye concentration.

Concentration	**Time**					
	0 (min.)	**50 (min.)**	**100 (min.)**	**150 (min.)**	**200 (min.)**	**250 (min.)**
10 ppm	0	23.02	38.90	50.68	65.72	72.66
15 ppm	0	16.94	39.62	53.4	66.19	81.28
20 ppm	**0**	**38.94**	**50.26**	**63.81**	**78.84**	**87.53**
25 ppm	0	24.89	34.39	48.33	68.81	78.81
50 ppm	0	15.12	26.95	35.28	48.54	60.51
100 ppm	0	12.19	16.68	18.17	24.34	35.55

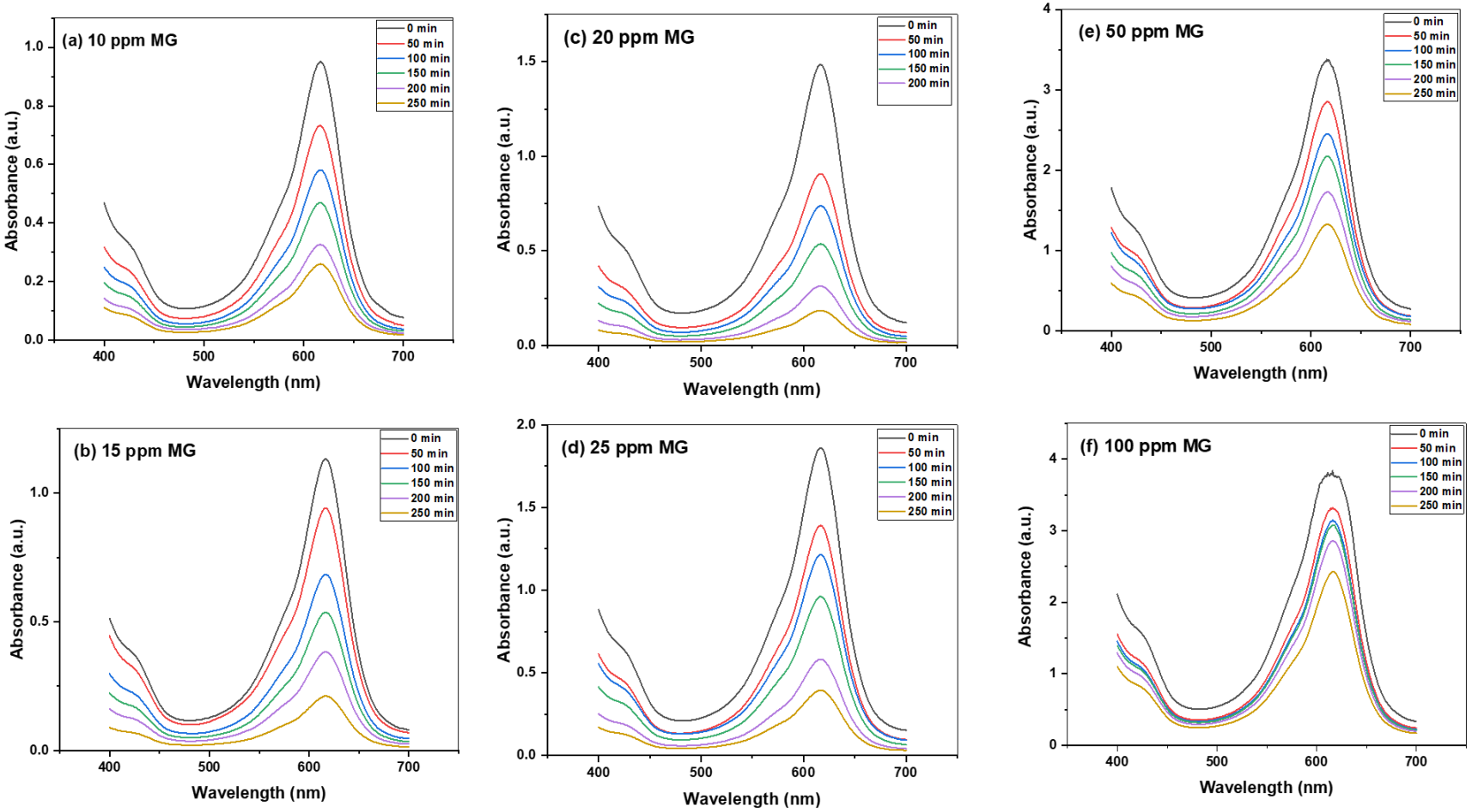

Figure 4.10: UV-Visible spectra of degradation of MG dye at different concentration (a) 10 ppm, (b) 15 ppm, (c) 20 ppm and (d) 25 ppm (e) 50 ppm (f) 100 ppm.

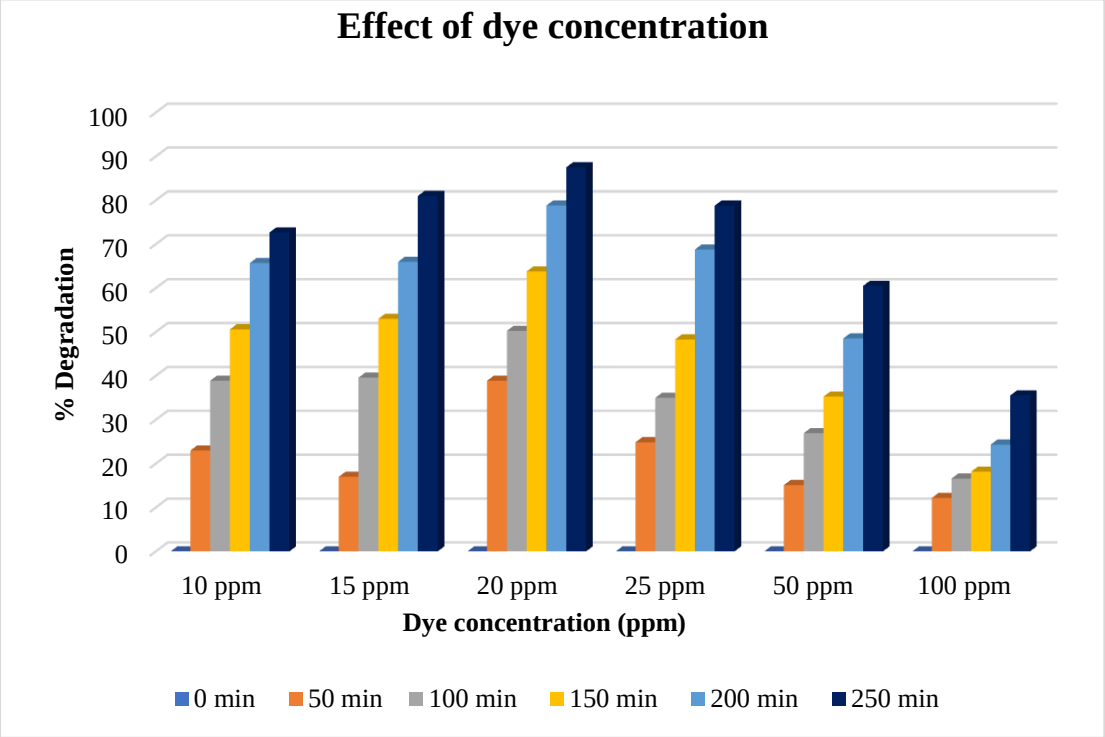

Figure 4.11: Percentage degradation vs dye concentration graph.

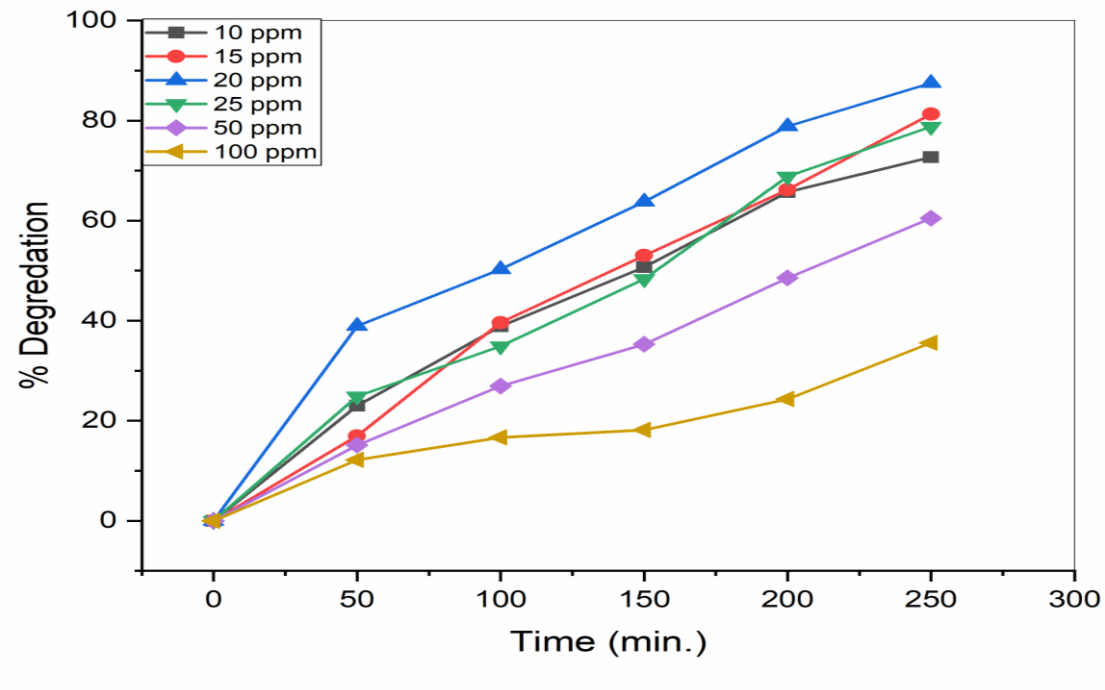

Figure 4.12: Percentage degradation Vs irradiation time graph at different dye concentration.

4.6.3. Effect of pH

The pH of a solution is a critical factor that can influence the degradation of organic dyes. Experiments on the degradation of MG solution at different pH levels (5, 7, 9, and 10) were carried out with catalyst load and dye concentration fixed at 150ppm and 20ppm, respectively. The degradation was shown to increase with increasing pH and decrease with increasing pH. The maximum amount of degradation obtained at pH 9, 91.63% of the dye was degraded after just one hour of irradiation. **Figure 4.13** illustrates the absorption spectra of dye at different pH. Another **figure 4.14 and figure 4.15** depicts the relation between dye degradation percentage vs pH and dye degradation percentage vs time, respectively.

The absorption of MG dye is determined by the catalyst's surface charge, which is determined by the catalyst's pzc (point zero charge). The pzc value of ZnO ranges from 8 to 9. Because MG is a cationic dye, the surface becomes positively charged at pH < pzc, repelling the dye molecules, whereas at pH > pzc, the surface becomes negatively charged, attracting the dye molecules. But at much higher pH the cationic form of Malachite green dye, transforms itself to neutral form, which has no attraction to the negatively charged solution **(Chen *et al.*, 2006)**.

Table 4.3: Percentage degradation of MG dye at different pH.

pH	**Time**				
	0 (min.)	**15 (min.)**	**30 (min.)**	**45 (min.)**	**60 (min.)**
pH 5	0	1.51	5.59	7.89	19.88
pH 7	0	18.82	37.06	44.70	57.40
pH 9	**0**	**28.76**	**71.75**	**78.34**	**91.63**
pH 10	0	24.22	44.70	50.62	59.51

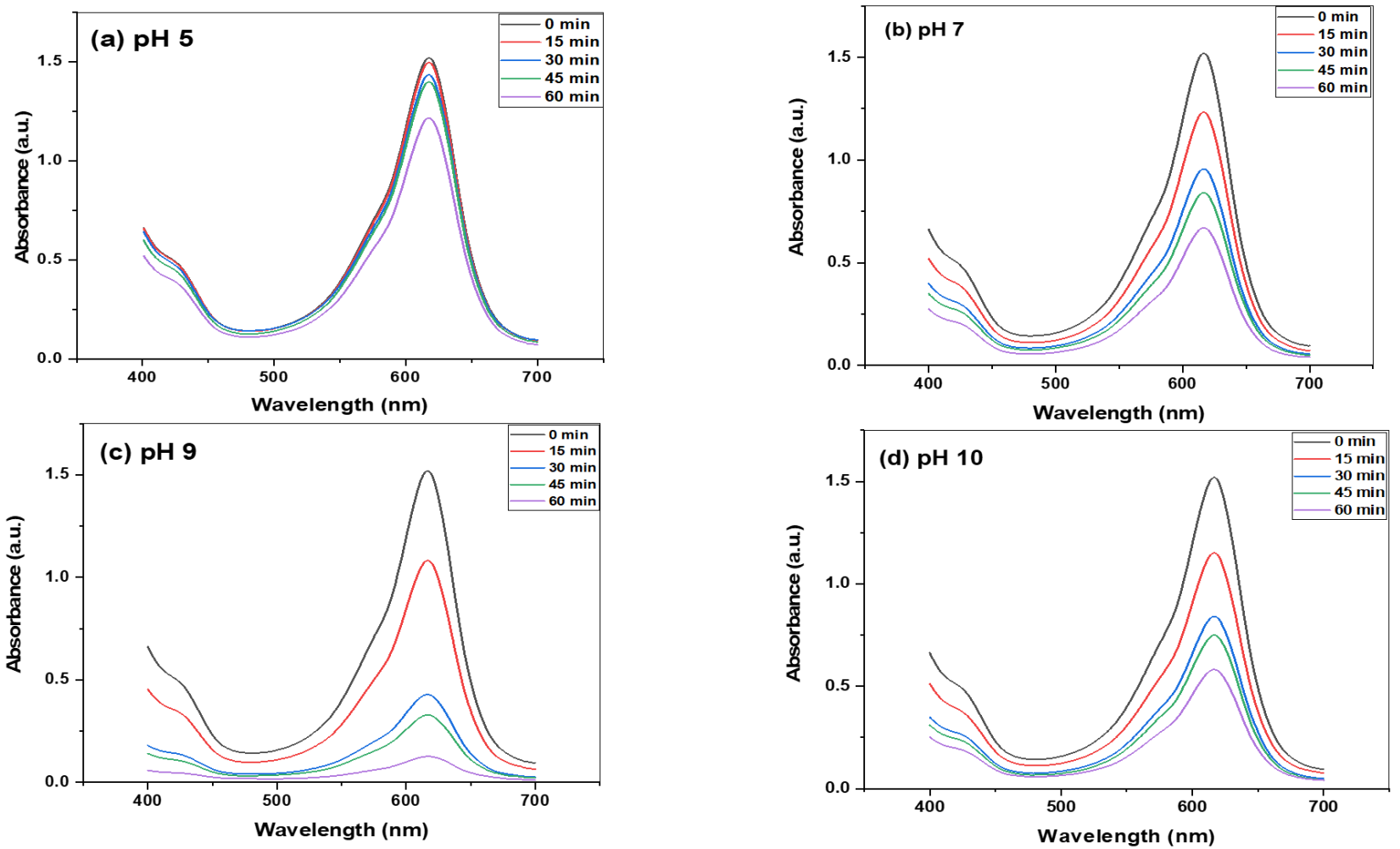

Figure 4.13: UV-Visible spectra of degradation of MG dye at different pH (a) 5, (b) 7, (c) 9, (d) 10.

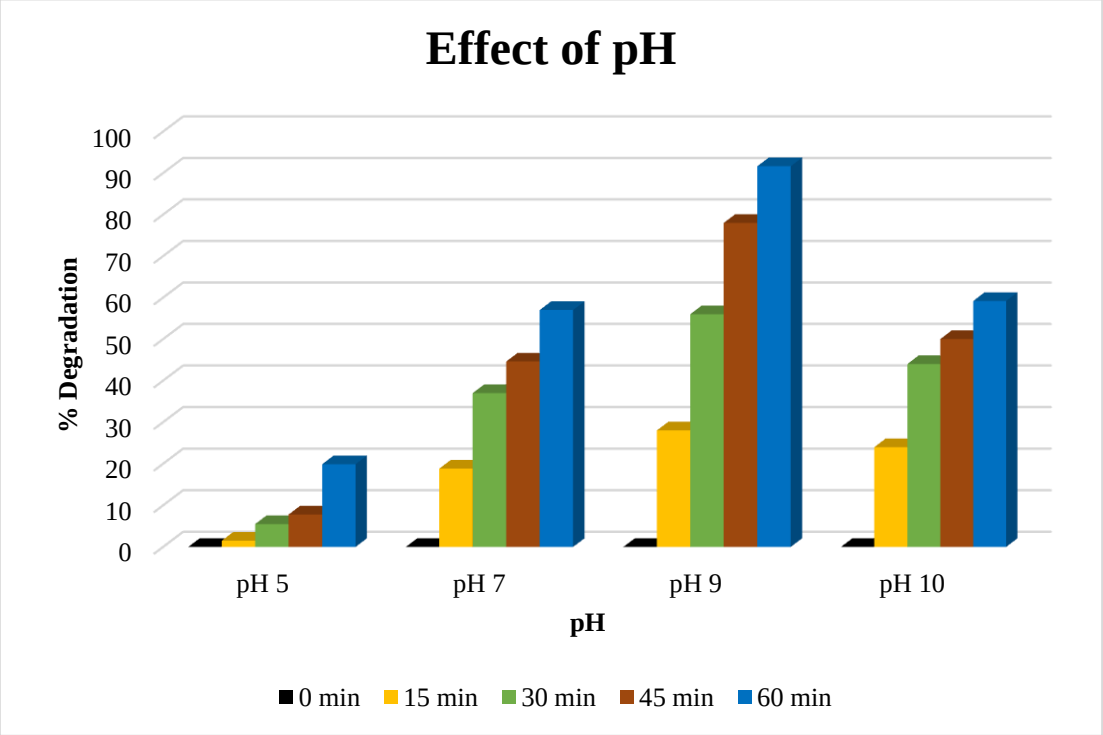

Figure 4.14: Percentage degradation vs pH.

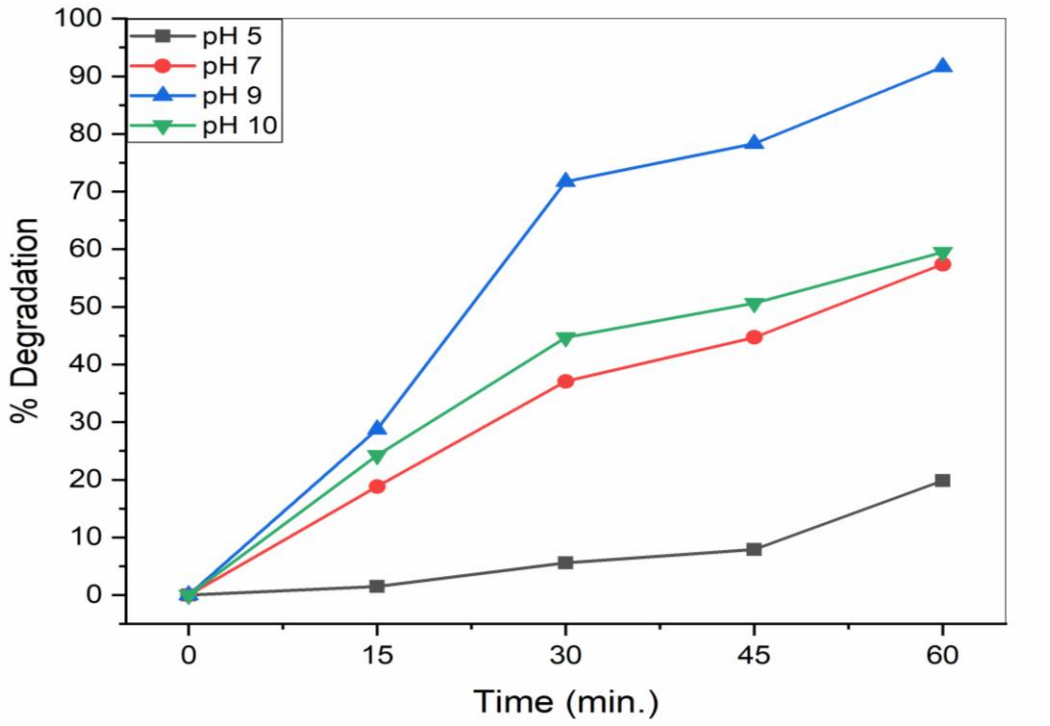

Figure 4.15: Percentage degradation Vs irradiation time graph at different pH.

Summary and Conclusions

Chapter 5 SUMMARY AND CONCLUSION

For better upcoming of nanotechnology, biosynthesis or green synthesis method should be used for the synthesis of nanoparticles to save environment and to avoid the use of dangerous chemical reducing agents and organic solvents. Due of the high durability, toxicity, and tendency to bioaccumulate in living species, dyes released in natural media have always been a major source of concern. Untreated discharged dyes block sunlight from reaching the bulk of the water system, thereby reducing the photosynthetic activity of aquatic system. The biological oxygen demand of contaminated water becomes considerably higher which pose significant environmental threat to the biota. In order to reduce the acute diverse effect of dyes, several techniques have been developed. The present study, titled **"Biosynthesis of zinc oxide nanoparticles employing fruits peel waste and their efficiency for degrading malachite green dye"** used fruits peel extract to synthesize zinc oxide nanoparticles. The extract of fruits peels worked as a reducing agent, as they are the rich source of polyphenols, flavonoids, alkaloids etc. No harsh chemicals were used during the entire study. The prepared fruits peel extract was mixed with the zinc oxide precursor in the ration of 1:5 for the synthesis of nanoparticles and during the reaction the optimum pH was maintained using NaOH. The obtained wet pale white precipitate was oven dried to procure nanoparticles. Several techniques were used to characterize synthesised nanoparticles, such as UV-Visible spectroscopy, Dynamic light scattering (DLS) analysis, Fourier transform infrared spectroscopy (FT-IR), X-ray diffraction (XRD) analysis, Field emission scanning electron microscopy (FE-SEM) and Energy dispersive X-ray analysis(EDX). 50ppm solution of obtained nanoparticles were prepared and sonicated for 15 min. to observe under UV- vis spectrophotometer. The UV-Vis spectrum of the sample gave a sharp peak at 378nm which is characterized peak for ZnO. The FT-IR was done to identify the functional group associated with ZnO NPs. FTIR revealed peaks at 3589.6, 3424.02, 2375.42, 1645.95, 1456.7, 1395.15, 863.95, and 674.76 cm^{-1} which corresponds to OH stretch, N-H stretch, alkynes stretching vibrations, C=O functional groups, amine (-NH)

vibration, alkanes bends and alkynes bends respectively. To characterized the structural properties of sample XRD was done. Diffraction peaks were found in sample. The planes (100), (002), (101), (102), (110), (103), (200), (112), and (201) confirm the formation of pure hexagonal wurtzite phase ZnO, which agrees well with the standard ICDD card No. 01-079-0205. Average hydrodynamic diameter of 162.1nm was reported through DLS analysis, which is significantly bigger than the sizes reported by FE-SEM. This deviation in nanoparticle sizes could be due to their polydisperse nature. According to FE-SEM images, few nanoparticles were in spherical shape and others were found to be in triangular shape. The size of the nanoparticles were found to be in the range of 60-100nm. EDX for ZnO NPs represented additional peaks for carbon and calcium along with the peaks of zinc and oxygen. The elements C and Ca are significant nutrients in fruits peel used, and the occurrence of their peaks in ZnO NP's EDX spectrum could have come from the extract used. Further, the photocatalytic activities were also performed to assess the degradation capabilities of synthesized ZnO NPs. Experiments were carried out using varying dosage of ZnO NPs (50ppm, 100ppm, 150ppm and 250ppm) while the dye concentration and pH were kept constant at 20ppm and 7, respectively. The minimum degradation of MG dye is observed at 50ppm ZnO NPs concentration, 63.07% and maximum degradation was observed with 150ppm concentration of ZnO NPs which is 93.08%. For varied dye concentrations of 10ppm, 15ppm, 20ppm, 25ppm, 50ppm and 100ppm, with fixed amount of ZnO NPs at 150ppm and pH 7, the influence of the initial dye concentration on the photocatalytic activity was investigated. As the dye concentration rises, the reaction between dye molecules and catalyst becomes easier, increasing the percentage of dye breakdown and after the dye concentration reaches an optimum level, the dye molecules cover the catalyst, preventing light from entering and creating a screen effect. At 20ppm concentration of MG dye, best degradation was observed. Experiments on the degradation of MG solution at different pH levels (5, 7, 9, and 10) were carried out with ZnO NPs load and dye concentration fixed at 150ppm and 20ppm, respectively. The degradation increased with increasing pH and decrease on further increasing pH. The maximum degradation was obtained at pH 9 (91.63%), just after one hour of irradiation.

The results of present study revealed that the use of natural and eco-friendly sources of reducing agents for the synthesis of ZnO NPs exhibit great photo-catalytic activity against MG dye and can be used to treat waste water. Therefore it can be stated that the utilization of biogenic process helps in designing of nanoparticles with the utmost stability as well as activity.

Literature Cited

LITERATURE CITED

Abdul Salam, H., Sivaraj, R. and Venckatesh, R. 2014. Green synthesis and characterization of zinc oxide nanoparticles from *Ocimum basilicum* L. var. purpurascens Benth.-Lamiaceae leaf extract. *Mat. Lett.,* 131: 16–18.

Agarwal, H., Rajeshkumar, S., Kumar, S. V., Ramaiah, A., Lakshmi, T. and Roopan, S. M. 2018. Biosynthesis of zinc oxide nanoparticles using *Mangifera indica* leaves and evaluation of their antioxidant and cytotoxic properties in lung cancer (A549) cells. *Enz. Micro. Tech*., 117: 91-95.

Aladpoosh, R. and Montazer, M. 2015. The role of cellulosic chains of cotton in biosynthesis of ZnO nanorods producing multifunctional properties: Mechanism, characterizations and features. *Car. Poly.,* 126: 122–129.

Ali, K., Dwivedi, S., Azam, A., Saquib, Q., Al-Said, M. S., Alkhedhairy, A. A. and Musarrat, J. 2016. Aloe vera extract functionalized zinc oxide nanoparticles as nanoantibiotics against multi-drug resistant clinical bacterial isolates. *J. Coll. and Int. Sci.,* 472: 145–156.

Ambika, S. and Sundrarajan, M. 2015. Green biosynthesis of ZnO nanoparticles using *Vitex negundo* L. extract: Spectroscopic investigation of interaction between ZnO nanoparticles and human serum albumin. *J. of Photochem. and Photo. Bio.,* 149: 143–148.

Anbuvannan, M., Ramesh, M., Viruthagiri, G., Shanmugam, N. and Kannadasan, N. 2015. *Anisochilus carnosus* leaf extract mediated synthesis of zinc oxide nanoparticles for antibacterial and photocatalytic activities. *Mat. Sci. Semicond. Proc*., 39: 621–628.

Anbuvannan, M., Ramesh, M., Viruthagiri, G., Shanmugam, N. and Kannadasan, N. 2015. Synthesis, characterization and photocatalytic activity of ZnO nanoparticles prepared by biological method. *Mol. Biomol. Spect.,* 143: 304-308.

Anju Devi, S., Singh, K. J. and Devi, K. N. 2020. A comparative study on the photocatalytic activity of eucalyptus leaf assisted green synthesized ZnO and chemically synthesized ZnO towards the degradation of malachite green dye. *Int. Ferro.*, 205(1): 38-51.

Aryan Rajan, Cherian, E. and Baskar, G. 2016. Biosynthesis of zinc oxide nanoparticles using Aspergillus fumigatus JCF and its antibacterial activity. *Int. J. Mod. Sci. Tech.*, 1: 52-7.

Azizi, S., Ahmad, M. B., Namvar, F. and Mohamad, R. 2014. Green biosynthesis and characterization of zinc oxide nanoparticles using brown marine macroalga *Sargassum muticum* aqueous extract. *Mat. Lett.*, 116: 275–277.

Binoj Nair and Pradeep, T. 2002. Coalescence of nanoclusters and formation of submicron crystallites assisted by Lactobacillus strains. *Cryst. Gr. Des.*, 2(4): 293-298.

Chaudhuri, S. K. and Malodia, L. 2017. Biosynthesis of zinc oxide nanoparticles using leaf extract of *Calotropis gigantea*: characterization and its evaluation on tree seedling growth in nursery stage. *App. Nano. sci.*, 7(8): 501–512.

Chen, J., Wu, C., Qiao, X., Wang, H., Tan, F. and Li, S. 2006. A novel chemical route to prepare ZnO nanoparticles. *Mat. Lett.*, 60(15): 1828-1832.

Cho, Bongsup P., Tianle Blankenship, Lonnie R. Moody, Joanna D. Churchwell, Mona Beland, Frederick A. Culp and Sandra J. 2003. Synthesis and Characterization of Demethylated Metabolites of Malachite Green and Leuco-malachite Green. *Chem. Res. Toxi.*, 16(3): 285–294.

Choi S. Mook, Seo H.M and Kim B.W. 2011. Synthesis and characterization of graphene surrounded nanoparticles by impregnation method with heat treatment in H_2 atmosphere. *Syn. Met.*, 161(21-22): 2404-2411.

De Oliveira, P. F. M., Torresi, R. M., Emmerling, F. and Camargo, P. 2020. Challenges and Opportunities in the Bottom-up Mechanochemical Synthesis of Noble Metal Nanoparticles. *J. of Mat. Chem.,*12: 4-18.

Devi, S. A., Singh, K. J. and Devi, K. N. 2020. A Comparative Study on the Photocatalytic Activity of Eucalyptus Leaf Assisted Green Synthesized ZnO and Chemically Synthesized ZnO towards the Degradation of Malachite Green Dye. *Int. Ferroelect.,* 205(1):38-51.

Dobrucka, R. and Długaszewska, J. 2016. Biosynthesis and antibacterial activity of ZnO nanoparticles using *Trifolium pratense* flower extract. *Saudi J. of Bio. Sci.,* 23(4): 517–523.

El-Gendy., Deemer, E., Fernandez-Delgado, O., Wang, H., Curry, M. L. and Noveron, J. C. 2019. Fe nanoparticles encapsulated in MOF-derived carbon for the reduction of 4-nitrophenol and methyl orange in water. *Cat. Comm.,* 130: 105753.

Elumalai, K. and Velmurugan, S. 2015. Green synthesis, characterization and antimicrobial activities of zinc oxide nanoparticles from the leaf extract of *Azadirachta indica* (L.). *Ap. Sur. Sci.,* 34(5): 329–336.

Elumalai, K., Velmurugan, S., Ravi, S., Kathiravan, V. and Ashokkumar, S. 2015. Green synthesis of zinc oxide nanoparticles using *Moringa oleifera* leaf extract and evaluation of its antimicrobial activity. *Mol. Biomol. Spect.,* 143: 158–164.

Fu, L. and Fu, Z. 2015. *Plectranthus amboinicus* leaf extract–assisted biosynthesis of ZnO nanoparticles and their photocatalytic activity. *Cer. Int.,* 41(2): 2492–2496.

Gorinstein, S., Park, Y. S., Namiesnik, J., Vearasilp, K., Leontowicz, H., Leontowicz, M., Barasch, D. 2014. Bioactive compounds and the antioxidant capacity in new kiwi fruit cultivars. *Food Chem.,* 165: 354-361.

Hadadian, M., Goharshadi, E. K., Fard, M. M. and Ahmadzadeh, H. 2018. Synergistic effect of graphene nanosheets and zinc oxide nanoparticles for effective adsorption of Ni (II) ions from aqueous solutions. *App. Phy. A.,* 124(3): 1-10.

Hadia, N. M. A., García-Granda, S. and García, J. R. 2014. Effect of the temperature on structural and optical properties of zinc oxide nanoparticles. *J. Nanosci. Nanotech.,* 14(7): 5443-5448.

Haslam, G. E., Adenle, A. A. and Lee, L. (2010). Global assessment of research and development for algae biofuel production and its potential role for sustainable development in developing countries. *En. Pol.,* 61: 182-195.

Hee, O. Rupa, Esrat Jahan, Anandapadmanaban G., Chokkalingam M., Li, Jin Feng, Markus, J., Soshnikova, V., Perez Z.E.J. and Yang Chun. 2018. Cationic and anionic dye degradation activity of Zinc oxide nanoparticles from *Hippophae rhamnoides* leaves as potential water treatment resource. *Optik.*, 4026(18): 32-48.

Heidi Van den Rul, Mondelaers, D., Van Bael, M. K. and Mullens, J. 2006. Water-based wet chemical synthesis of (doped) ZnO nanostructures. *J. Sol-gel Sci. Tech., 39*(1): 41-47.

Hiroyuki Usui, Shimizu, Y., Sasaki, T. and Koshizaki, N. 2004. Photoluminescence of ZnO nanoparticles prepared by laser ablation in different surfactant solutions. *J. Phy. Chem. B.*, 109(1): 120-124.

Huang L, Weng X, Chen Z, Mallavarapu M and Naidu R. 2014. Synthesis of iron-based nanoparticles using oolong tea extract for the degradation of malachite green. *Spectrochim. Acta. Mol. Biomol. Spectro.,* 117: 801-804.

Jafarirad, S., Mehrabi, M., Divband, B. and Kosari-Nasab, M. 2016. Bio fabrication of zinc oxide nanoparticles using fruit extract of *Rosa canina* and their toxic potential against bacteria: A mechanistic approach. *Mat. Sci. and Eng.,* 59: 296–302.

Jamkhande, P. G., Ghule, N. W., Bamer, A. H. and Kalaskar, M. G. 2019. Metal nanoparticles synthesis: An overview on methods of preparation, advantages and disadvantages and applications. *J. Drug Del. Sci. and Tech.,* 10: 11-74.

Jassal V, Shanker U and Gahlot U. 2016. Green synthesis of some iron oxide nanoparticles and their interaction with 2-Amino, 3-Aminoand 4-Aminopyridines. *Mat. Tod. Proc.,* 3: 1874-1882.

Jiang, X., Liu, Y., Gao, Y., Zhang, X. and Shi, L. 2010. Preparation of one-dimensional nanostructured ZnO. *Parti.*, 8(4): 383–385.

Jin, W., Lee, I.-K., Kompch, A., Dörfler, U. and Winterer, M. 2007. Chemical vapor synthesis and characterization of chromium doped zinc oxide nanoparticles. *J. Euro. Cer. Soci.,* 27(13-15): 4333–4337.

Khan, S. H. and Pathak, B. 2020. Zinc oxide based photocatalytic degradation of persistent pesticides: A comprehensive review. *Envi. Nanotech. Moni. Man.,* 13: 100290.

Krupa, A. N. D. and Vimala, R. 2016. Evaluation of tetraethoxysilane (TEOS) sol–gel coatings, modified with green synthesized zinc oxide nanoparticles for combating microfouling. *Mat. Sci. and Eng.,* 61: 728–735.

Mallikarjunaswamy, C., Ranganatha, V. L., Nithin, K. S., Khanum and S. A., Nagaraju, G. 2019. Zinc oxide nanoparticles: A significant review on synthetic strategies, characterization and applications. *AIP Conf. Pro.,* 10: 11-74.

Marco Stoller and Ochando-Pulido, J. M. 2020. ZnO Nano-particles production intensification by means of a spinning disk reactor. *Nanomat.,* 10(7): 1321.

Meena, M., Senthilkumar, N., Ganapathy, M., Arulraj, A., Vimalan, M. and Potheher, I. V. 2018. Two step synthesis of ZnO/Ag and ZnO/Au core/shell nanocomposites: structural, optical and electrical property analysis. *J. All. Comp.,* 750: 171-181.

Nagarajan, S. and Arumugam Kuppusamy, K. 2013. Extracellular synthesis of zinc oxide nanoparticle using seaweeds of gulf of Mannar, India. *J. of Nano-Biotech.,* 11(1): 39.

Nair, B. and Pradeep, T. 2002. Coalescence of Nanoclusters and Formation of Submicron Crystallites Assisted by Lactobacillus Strains. *Cryst. Gro. Dsg.,* 2(4): 293–298.

Nava, O. J., Soto-Robles, C. A., Gómez-Gutiérrez, C. M., Vilchis-Nestor, A. R., Castro-Beltrán, A., Olivas, A. and Luque, P. A. 2017. Fruit peel extract mediated green synthesis of zinc oxide nanoparticles. *J. of Mol. Str.,* 1147: 1-6.

Nekouei F, Noorizadeh H, Nekouei S, Asif M, Tyagi I, Agarwal S and Gupta VK. 2016. Removal of malachite green from aqueous solutions by cuprous iodide–cupric oxide nano-composite loaded on activated carbon as a new sorbent for solid phase extraction: isotherm, kinetics and thermodynamic studies. *J. Mol. Liq.,* 213: 360-368.

Pragati Jamdagni, Khatri, P. and Rana, J. S. 2016. Green synthesis of zinc oxide nanoparticles using flower extract of Nyctanthes arbor-tristis and their antifungal activity. *J. King Saud Uni.-Sci.,* 30(2): 168-175.

Prasad, A. R., Garvasis, J., Oruvil, S. K. and Joseph, A. 2019. Bio-inspired green synthesis of zinc oxide nanoparticles using Abelmoschus esculentus mucilage and selective degradation of cationic dye pollutants. *J. Phy. Chem. So.*, 127: 265-274.

Rajiv, P., Rajeshwari, S. and Venckatesh, R. 2013. Bio-Fabrication of zinc oxide nanoparticles using leaf extract of *Parthenium hysterophorus* L. and its size-dependent antifungal activity against plant fungal pathogens. *Mol. and Biomol. Spect.,* 112: 384-387.

Rambabu, K., Bharath, G., Banat, F. and Show, P. L. 2021. Green synthesis of zinc oxide nanoparticles using Phoenix dactylifera waste as bioreductant for effective dye degradation and antibacterial performance in wastewater treatment. *J. haz. Mat.*, 402: 123560.

Ramesh, M., Anbuvannan, M. and Viruthagiri, G. 2015. Green synthesis of ZnO nanoparticles using *Solanum nigrum* leaf extract and their antibacterial activity. *Mol. and Bio. Spect.,* 136: 864-870.

Romelle, F. D., Rani, A. and Manohar, R. S. 2016. Chemical composition of some selected fruit peels. *European Journal of Food Science and Technology*, *4*(4), 12-21.

Saha S. and Pal A. 2014. Microporous assembly of MnO_2 nanosheets for malachite green degradation. *Sep. Purif. Techno.,* 134: 26-36.

Sangeeta Nagarajan and Kuppusamy, K. A. 2013. Extracellular synthesis of zinc oxide nanoparticle using seaweeds of gulf of Mannar, India. *J. Nanobiotech.,* 11(1): 1-11.

Saratale R.G., Saratale G.D. and Shin H.S. 2018. New insights on the green synthesis of metallic nanoparticles using plant and waste biomaterials: current knowledge, their agricultural and environmental applications. *Environ. Sci. Pollut. Res.,* 25: 10164-10183.

Sepulveda-Guzman, S., Reeja-Jayan, B., de la Rosa, E., Torres-Castro, A., Gonzalez-Gonzalez, V. and Jose-Yacaman, M. 2009. Synthesis of assembled ZnO structures by precipitation method in aqueous media. *Mat. Chem. and Phy*., 115(1): 172-178.

Shankar, S. and Rhim, J. W. 2017. Facile approach for large-scale production of metal and metal oxide nanoparticles and preparation of antibacterial cotton pads. *Carbo. Poly.,* 163: 137-145.

Sharma, S., Hasan, A., Kumar, N. and Pandey, L. M. 2018. Removal of methylene blue dye from aqueous solution using immobilized Agrobacterium fabrum biomass along with iron oxide nanoparticles as biosorbent. *Env. Sci. Poll. Res., 25*(22): 21605-21615.

Singhai, M., Chhabra, V., Kang, P. and Shah, D. O. 1997. Synthesis of ZnO nanoparticles for varistor application using Zn-substituted aerosol ot microemulsion. *Mat. Res. Bull.,* 32(2): 239-247.

Skapin, S. D., Dražič, G. and Orel, Z. C. 2007. Microstructure of nanoscale zinc oxide crystallites. *Mat. Lett.,* 61(13): 2783-2788.

Stoller, M. and Ochando-Pulido, J. M. 2020. ZnO Nano-Particles Production Intensification by Means of a Spinning Disk Reactor. *Nanomat.,* 10(7): 1321.

Sukri, S. N. A. M., Shameli, K., Wong, M. M. T., Teow, S. Y., Chew, J. and Ismail, N. A. 2019. Cytotoxicity and antibacterial activities of plant-mediated synthesized zinc oxide (ZnO) nanoparticles using Punica granatum (pomegranate) fruit peels extract. *J. Mole. Str., 1189*: 57-65.

Sultana, J., Siddique, M. N. A. and Abdullah, M. R. 2015. Fertilizer recommendation for agriculture: practice, practicalities and adaptation in Bangladesh and Netherlands. *Int. J. Bus. Manag. So. Res.*, 1(1): 21-40.

Sundrarajan, M., Ambika, S. and Bharathi, K. 2015. Plant-extract mediated synthesis of ZnO nanoparticles using *Pongamia pinnata* and their activity against pathogenic bacteria. *Adv. Pow. Tech.,* 26(5): 1294-1299.

Susan Azizi, Ahmad, M., Mahdavi, M. and Abdolmohammadi, S. 2013. Preparation, characterization and antimicrobial activities of ZnO nanoparticles/cellulose nanocrystal nanocomposites. *BioRes*., 8(2): 1841-1851.

Thema, F. T., Manikandan, E., Dhlamini, M. S. and Maaza, M. 2015. Green synthesis of ZnO nanoparticles via *Agathosma betulina* natural extract. *Mat. Lett.,* 161: 124-127.

Tripathi, R. M., Bhadwal, A. S., Gupta, R. K., Singh, P., Shrivastav, A. and Shrivastav, B. R. 2014. ZnO nanoflowers: Novel biogenic synthesis and enhanced photocatalytic activity. *J. of Photochem. and Photobio.,* 141: 288-295.

Usui, H., Shimizu, Y., Sasaki, T. and Koshizaki, N. 2005. Photoluminescence of ZnO Nanoparticles Prepared by Laser Ablation in Different Surfactant Solutions. *The J. Phy. Chem.,* 109(1): 120-124.

Vafaee, M. and Ghamsari, M. S. 2007. Preparation and characterization of ZnO nanoparticles by a novel sol–gel route. *Mat. Lett.,* 61(14-15): 3265-3268.

Valdez-Vazquez, I., Torres-Aguirre, G. J., Molina, C. and Ruiz-Aguilar, G. M. 2016. Characterization of a lignocellulolytic consortium and methane production from untreated wheat straw: dependence on nitrogen and phosphorous content. *BioRes.,* 11(2): 4237-4251.

Van den Rul, H., Mondelaers, D., Van Bael, M. K. and Mullens, J. 2006. Water-based wet chemical synthesis of (doped) ZnO nanostructures. *J. Sol-Gel Sci. Tech.,* 39(1): 41-47.

Vanathi, P., Rajiv, P., Narendhran, S., Rajeshwari, S., Rahman, P. K. S. M. and Venckatesh, R. 2014. Biosynthesis and characterization of phyto-mediated zinc oxide nanoparticles: A green chemistry approach. *Mat. Lett.,* 134: 13-15.

Wei Jin, Lee, I. K., Kompch, A., Dörfler, U. and Winterer, M. 2007. Chemical vapor synthesis and characterization of chromium doped zinc oxide nanoparticles. *J. Euro. Cer. Soc.*, 27(13-15): 4333-4337.

Wu, Yan Zeng, Shenliang Wang, Feifeng Megharaj, Mallavarapu Naidu, Ravendra Chen and Zuliang. 2015. Heterogeneous Fenton-like oxidation of malachite green by iron-based nanoparticles synthesized by tea extract as a catalyst. *Sep. Puri. Tech.*, 154: 161-167.

Xiuping Jiang, Liu, Y., Gao, Y., Zhang, X. and Shi, L. 2010. Preparation of one-dimensional nanostructured ZnO. *Part.*, 8(4): 383-385.

YANG, G. 2006. Laser ablation in liquids: Applications in the synthesis of nanocrystals. *Prog. Mat. Sci.,* 52(4): 648–698.

Yanli Gao, Xu, D., Ren, D., Zeng, K. and Wu, X. (2020). Green synthesis of zinc oxide nanoparticles using Citrus sinensis peel extract and application to strawberry preservation: A comparison study. *LWT*, 126: 109297.

Yuvakkumar, R., Suresh, J., Nathanael, A. J., Sundrarajan, M. and Hong, S. I. 2014. Novel green synthetic strategy to prepare ZnO nanocrystals using rambutan (*Nephelium lappaceum* L.) peel extract and its antibacterial applications. *Mat. Sci. and Eng.*, 41: 17–27.

CURRICULUM VITAE

Name	**:**	Mr. Deepak Bahuguna	**Phone Number**	**:**	9610315864
Mailing Address	**:**	Room no.-1550, Sector-03 Pushp Vihar, Saket, Delhi	**Permanent Address**	**:**	H. No.- 47, Deghat, Uttarakhand
E-mail	**:**	Deepakbahuguna5@gmail.com			
Career Objective	**:**	To expand my learnings, knowledge and skills.			

Educational Qualification

Sr. No.	Examination Passed	Institution	Year	Percentage/CGPA
1.	M.Sc.	GBPUA&T, Pantnagar	2021	Pursuing
2.	B.Sc.	Amity University, Noida	2019	7.78
3.	Intermediate	K.V. A.A.I. Rangpuri	2014	62.3%
4.	High School	K.V. A.A.I. Rangpuri	2012	8.4

Specialization: Major: Environmental Science Minor: Nil

Publication: Nil

Conference/Seminars/Workshops/Training Attended: 3

List of papers presented in conference/seminar during degree programme: 0

Software Skills: MS Word, MS Excel, MS Power Point.

Professional Skills: Critical thinking and problem solving.

Professional Affiliations (Membership, etc.,): Teaching assistant

Awards/Honours/Achievements: Teaching assistantship scholarship, Internship at IRMA Anand.

(Deepak Bahuguna)

Place: Pantnagar

Date: September, 2021

Name	:	Deepak Bahuguna	**Id. No.**	:	55546
Sem. and year of admission	:	1st, 2019-20	**Degree**	:	M.Sc.
Department	:	Environmental Science			
Major	:	Environmental Science			
Thesis title	:	BIOSYNTHESIS OF ZINC OXIDE NANOPARTICLES EMPLOYING FRUITS PEEL WASTE AND THEIR EFFICIENCY FOR DEGRADING MALACHITE GREEN DYE			
Page No.	:	53	**Advisor**	:	**Dr. Shweta Saraswat**

ABSTRACT

One of the major challenges in the 21st century is to satisfy the human requirement of clean water. Discharge of several untreated chemical and biological pollutants has deteriorated the drinking water quality. To minimize the effects of toxic chemicals, biological reduction agents are being explored worldwide for nanoparticle fabrication. The present study was undertaken to assess the synthesis of Zinc oxide nanoparticles (ZnO NPs) from multiple fruits peel waste and their application for degradation of Malachite green dye. The fruit peels contain active biomolecules such as flavonoids, phenolic acids and alkaloids in large quantity. The synthesized nanoparticles were characterized using various techniques such as UV-Vis Spectroscopy, FT-IR), DLS, XRD analysi, FE-SEM and EDX. Precursors used in synthesis were Zinc nitrate hexahydrate and NaOH, method used was bio-reduction and the prepared nanoparticles were employed under different parameters for degradation of malachite green dye. The size range of nanoparticles obtained was within the range of 60-100nm as reported by FE-SEM. X-ray diffraction studies confirmed the crystalline nature of the nanoparticles. The maximum malachite green degradation, about 93.08% was obtained at pH 7, ZnO NPs concentration 150ppm and dye concentration 20ppm under solar irradiation. The results revealed that the pretreated mixed fruit peel waste is a promising resource for synthesizing nanoparticles due to the phytochemicals that act as good reducing and stabilizing agent, and can be further employed for the sake of environmental pollution remediation.

(Shweta Saraswat)
Advisor

(Deepak Bahuguna)
Author

नाम	: दीपक बहुगुणा	**परिचयांक**	: 55546
षट्मास एवं प्रवेष वर्ष	: प्रथम, 2019-2020	**उपाधि**	: एम0एस0सी0
विभाग	: पर्यावरण विज्ञान		
प्रमुख विषय	: पर्यावरण विज्ञान		
शोध का शीर्षक	: फलों के छिलकों के अपशिष्ट से जिंक ऑक्साइड नैनोकणों का जैवसंश्लेषण तथा मैलाकाइट ग्रीन डाई को नष्ट करने की उनकी क्षमता		
पृष्ठ संख्या	:	**सलाहकार**	: डॉ० श्वेता सारस्वत

सारांश

२१वीं सदी में सबसे बड़ी चुनौतियों में से एक स्वच्छ पानी की मानवीय आवश्यकता को पूरा करना है। कई अनुपचारित रासायनिक और जैविक प्रदूषकों के निर्वहन ने पीने के पानी की गुणवत्ता को खराब कर दिया है। जहरीले रसायनों के प्रभाव को कम करने के लिए, दुनिया भर में विभिन्न नैनोकणों के निर्माण की खोज की जा रही है। वर्तमान अध्ययन कई फलों के छिलके के कचरे से जिंक ऑक्साइड नैनोपार्टिकल्स (ZnO NPs) के संश्लेषण तथा उनके द्वारा मैलाकाइट ग्रीन डाई के निम्नीकरण का आकलन करने के लिए किया गया था। फलों के छिलकों में सक्रिय बायोमोलेक्यूल्स जैसे फ्लेवोनोइड्स, फेनोलिक एसिड और एल्कलॉइड बड़ी मात्रा में होते हैं। संश्लेषित नैनोकणों की विशेषता यूवी-विज़ स्पेक्ट्रोस्कोपी, FTIR, DLS, XRD विश्लेषण, FE-SEM तथा EDX जैसी विभिन्न तकनीकों का उपयोग करके पता की गई। संश्लेषण में उपयोग किए जाने वाले रासायन जिंक नाइट्रेट हेक्साहाइड्रेट और NaOH थे तथा तैयार नैनोकणों को मैलाकाइट ग्रीन डाई के निम्नीकरण के लिए, विभिन्न मापदंडों के तहत नियोजित किया गया था। FE-SEM रिपोर्ट के अनुसार प्राप्त नैनोकणों की आकार सीमा 60-100nm के भीतर थी तथा XRD अध्ययनों ने नैनोकणों की क्रिस्टलीय प्रकृति की पुष्टि की। अधिकतम मैलाकाइट ग्रीन क्षरण pH-7, ZnO NPs मात्रा 150ppm और डाई मात्रा 20ppm, नियमित विकिरण के तहत प्राप्त किया गया। सूर्य के प्रकाश मे, संश्लेषित ZnO NPs ने 250 मिनट मे 93.08% MG डाई को प्रभावी ढंग से नष्ट किया। परिणामों से सिद्ध होता है, कि मिश्रित फलों के छिलके का अपशिष्ट नैनोकणों के संश्लेषण के लिए एक आशाजनक संसाधन है तथा इसे पर्यावरण प्रदूषण निवारण के लिए आगे नियोजित किया जा सकता है।

श्वेता सारस्वत

(श्वेता सारस्वत)
सलाहकार

दीपक बहुगुणा

(दीपक बहुगुणा)
लेखक